Aerosol and Air Quality Research, 16: 2581–2602, 2016

ISSN: 1680-8584 print / 2071-1409 online
doi: 10.4209/aaqr.2016.08.0350

Satellite-Surface Perspectives of Air Quality and Aerosol-Cloud Effects on the Environment: An Overview of 7-SEAS/BASELInE

Si-Chee Tsay[1*], Hal B. Maring[2], Neng-Huei Lin[3,5], Sumaman Buntoung[4], Somporn Chantara[5], Hsiao-Chi Chuang[6], Philip M. Gabriel[7], Colby S. Goodloe[1], Brent N. Holben[1], Ta-Chih Hsiao[3], N. Christina Hsu[1], Serm Janjai[4], William K.M. Lau[8], Chung-Te Lee[3], Jaehwa Lee[1,8], Adrian M. Loftus[1,8], Anh X. Nguyen[9], Cuong M. Nguyen[10], Shantanu K. Pani[3], Peter Pantina[1,11], Andrew M. Sayer[1,12], Wei-Kuo Tao[1], Sheng-Hsiang Wang[3], Ellsworth J. Welton[1], Wan Wiriya[5], Ming-Cheng Yen[3]**

[1] *NASA Goddard Space Flight Center, Greenbelt, Maryland, USA*
[2] *NASA Headquarters, Washington, DC, USA*
[3] *National Central University, Chung-Li, Taiwan*
[4] *Faculty of Science, Silpakorn University, Nakhon Pathom, Thailand*
[5] *Faculty of Science, Chiang Mai University, Chiang Mai, Thailand*
[6] *School of Respiratory Therapy, Taipei Medical University, Taipei, Taiwan*
[7] *General Analytics, LLC, Fort Collins, Colorado, USA*
[8] *ESSIC, University of Maryland, College Park, Maryland, USA*
[9] *Vietnam Academy of Science and Technology, Hanoi, Vietnam*
[10] *National Research Council of Canada, Ottawa, Canada*
[11] *Science Systems and Applications, Inc., Lanham, Maryland, USA*
[12] *GESTAR/USRA, Columbia, Maryland, USA*

ABSTRACT

The objectives of 7-SEAS/BASELInE (Seven SouthEast Asian Studies/Biomass-burning Aerosols & Stratocumulus Environment: Lifecycles & Interactions Experiment) campaigns in spring 2013–2015 were to synergize measurements from uniquely distributed ground-based networks (e.g., AERONET, MPLNET) and sophisticated platforms (e.g., SMARTLabs, regional contributing instruments), along with satellite observations/retrievals and regional atmospheric transport/chemical models to establish a critically needed database, and to advance our understanding of biomass-burning aerosols and trace gases in Southeast Asia (SEA). We present a satellite-surface perspective of 7-SEAS/BASELInE and highlight scientific findings concerning: (1) regional meteorology of moisture fields conducive to the production and maintenance of low-level stratiform clouds over land, (2) atmospheric composition in a biomass-burning environment, particularly tracers/markers to serve as important indicators for assessing the state and evolution of atmospheric constituents, (3) applications of remote sensing to air quality and impact on radiative energetics, examining the effect of diurnal variability of boundary-layer height on aerosol loading, (4) aerosol hygroscopicity and ground-based cloud radar measurements in aerosol-cloud processes by advanced cloud ensemble models, and (5) implications of air quality, in terms of toxicity of nanoparticles and trace gases, to human health. This volume is the third 7-SEAS special issue (after *Atmospheric Research,* vol. 122, 2013; and *Atmospheric Environment,* vol. 78, 2013) and includes 27 papers published, with emphasis on air quality and aerosol-cloud effects on the environment. BASELInE observations of stratiform clouds over SEA are unique, such clouds are embedded in a heavy aerosol-laden environment and feature characteristically greater stability over land than over ocean, with minimal radar surface clutter at a high vertical spatial resolution. To

* Corresponding author.
Tel.: +13016146188; Fax: +13016146307
E-mail address: si-chee.tsay@nasa.gov
** Corresponding author.
Tel./Fax: +886-3-4254069
E-mail address: nhlin@cc.ncu.edu.tw

facilitate an improved understanding of regional aerosol-cloud effects, we envision that future *BASELInE-like* measurement/modeling needs fall into two categories: (1) efficient yet critical *in-situ* profiling of the boundary layer for validating remote-sensing/retrievals and for initializing regional transport/chemical and cloud ensemble models, and (2) fully utilizing the high observing frequencies of geostationary satellites for resolving the diurnal cycle of the boundary-layer height as it affects the loading of biomass-burning aerosols, air quality and radiative energetics.

Keywords: 7-SEAS; BASELInE; Biomass-burning; Air Quality; Aerosol; Cloud.

BACKGROUND AND MOTIVATION

Air quality, as a measure of natural and anthropogenic emissions of pollutants into the atmosphere, is receiving increasing global attention. It correlates with the health of humans and ecosystems and is also a reflector of meteorological processes occurring predominantly on local to regional scales. The associated particulate matter (PM) and trace gases (e.g., O_3, CO_2, NO_2), acting as radiative forcing agents and participating in numerous atmospheric processes, including photochemistry, chemical transformation, convection, and cloud nucleation/retroaction, alter weather and climate (*cf.* IPCC, 2013; and references therein). In addition, increased understanding of the effects played by air quality on the health of humans and ecosystems has underscored the benefits of decreasing exposure to fine PM and toxic gaseous pollutants. Such contaminants are the leading environmentally-related cause of premature mortality worldwide (*cf.* Lelieveld *et al*., 2015; and references therein). In addition, the connections of air quality with global climate change rest in the synergy between observations and modeling efforts. The latter relate forcings that account for the feedbacks between regional air quality and climate. As the global population continues to grow, the demands on energy and land cover/use will increase, as will industrial/societal activities. Hence, the need to monitor and understand air quality is urgent and pervasive.

Prior to the advent of satellite observations, air quality monitoring had relied heavily on surface observations and modeling to develop mitigation strategies. Since 1997, NASA's Earth Observing System (EOS, 1999; EOS Mission Profiles, http://eospso.gsfc.nasa.gov), among other programs, has been successfully operating a series of low-Earth-orbit (LEO) satellites to further the understanding of the Earth-atmosphere system and the effects of natural and anthropogenic changes on the global environment. This development has been advanced in lockstep with surface/suborbital observations and modeling efforts. Furthermore, as illustrated in Fig. 1, field campaigns *simultaneously* serve to unite the aforementioned complementary components – satellite measurements and retrievals, ground-based observations and networks, and comprehensive climate

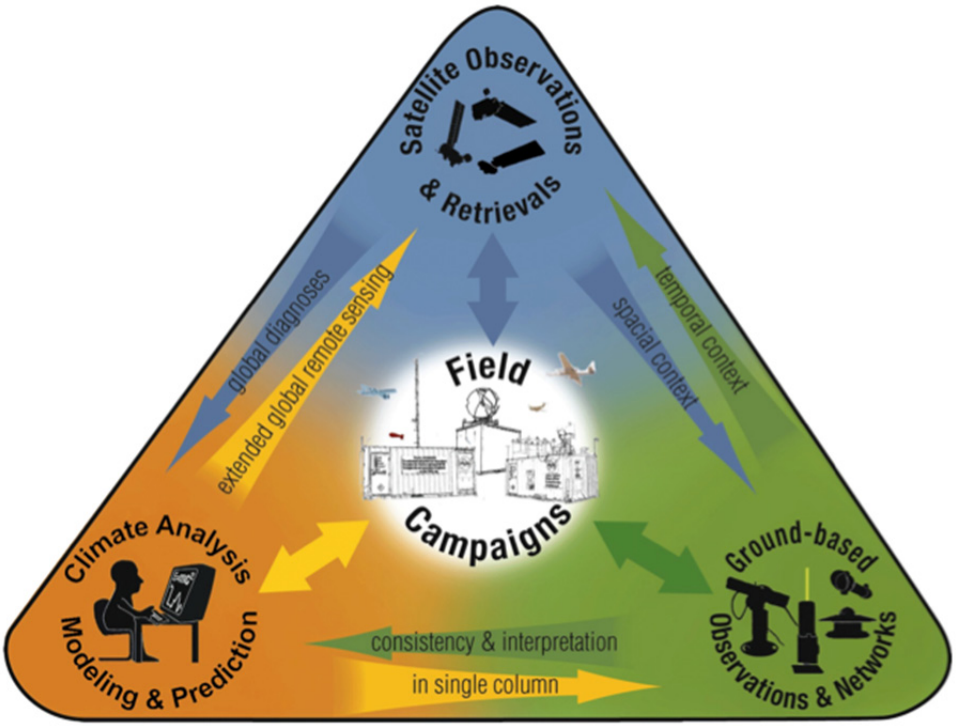

Fig. 1. A comprehensive strategy to integrate the individual components that comprise the research activities for understanding the Earth-atmosphere system; the arrows signify the complementary roles and the strengths between components.

analyses and modeling & prediction – in near real-time for a more incisive understanding of the Earth-atmosphere system. Additional benefits of surface and suborbital observations provide calibration/validation activities that are of paramount importance for satellite measurements to attain their full potential.

While LEO satellites have demonstrated observational capability of the critical constituents affecting air quality, their ability to observe fine spatial structures at a high temporal resolution is insufficient to monitor air quality events that can develop in less than a day. Thus, geostationary (GEO) satellites can provide observations fulfilling this requirement. As portrayed in Table 1, the wave of the future (e.g., the Decadal Survey, http://decadal.gsfc.nasa.gov/, among other space programs) points to second-generation sensors from GEO platforms, which have evolved largely from mature LEO predecessors. These will constitute invaluable tools for monitoring, diagnosing and projecting air quality. Moreover, ground-based observations over a distributed network, emphasizing the richness in spectral-temporal (remote sensing) and physiochemical (*in-situ*) sampling, complement satellites for essential information. In turn, critical information content for comparisons is made available that confirms quantitatively the usefulness of the integrated surface, aircraft and satellite (particularly GEO) measurements, as well as validating chemical-transport and assimilation models. This is crucial for advancing our state of understanding of the complex aerosol-cloud-radiation

Table 1. Categories of currently available and forthcoming tropospheric aerosol/cloud spaceborne sensors including example instruments (abbreviation, *cf.* Appendix), with their specifications (relevant data and spatial/temporal sampling), and duration (or expected launch time) of operations.

	Category	Instrument	Specifications		Duration
			Relevant data	Coverage	
LEO	Spectral imager	AVHRR MODIS Terra/Aqua VIIRS	Broad-swath aerosol and cloud	2900 km swath, various overpass times 2330 km swath, ~10:30/~1:30 local time 3040 km swath, ~1:30 local time	1978+ 2000+ 2012+
	Multiangle imager	MISR SLSTR	Narrower-swath aerosol and cloud; more constraints on size and absorption than spectral	360 km swath, ~10:30 local time 740 km dual-view swath, 10:00 local time	2000+ 2016+
	Polarization and multiangle imager	POLDER S-GLI	Greatest information content for aerosol and cloud retrievals	2400 km swath, ~1:30 local time 1400 (imager)/1150 km (polarized multiangle) swath, 10:30 local time	2004–2013 Exp. 2017
	UV-focused imaging spectrometer	OMI OMPS nadir TropOMI	Particularly sensitive to UV-absorbing aerosols; some trace gas information	2600 km swath, ~1:30 local time 2800 km swath, ~1:30 local time 2600 km swath, ~1:30 local time	2004+ 2012+ Exp. 2016
	Thermal-focused spectrometer	AIRS IASI CrIS	Mostly used for clouds and ash/dust aerosols; some trace gas information	1650 km swath, ~1:30 local time 2200 km swath, ~9:30 local time 2200 km swath, ~1:30 local time	2002+ 2006+ 2012+
	Lidar	CALIOP/CALIPSO ALADIN/ADM ATLID/EarthCARE	Vertical profiles of aerosols and clouds	Curtain profile, ~1:30 local time Curtain profile, ~6:00 local time Curtain profile, ~2:00 local time	2006+ Exp. 2016 Exp. 2018
	Radar	CPR/CloudSat DPR/GPM CPR/EarthCARE	Vertical profiles of clouds and precipitation	Curtain profile, ~1:30 local time 245 km swath, precessing orbit Curtain profile, ~2:00 local time	2006+ 2014+ Exp. 2018
	Microwave radiometer	SSM/I GMI	Broad-swath for clouds and precipitation	1707 km swath, various local times 904 km swath, precessing orbit	1987+ 2014+
GEO	Ocean color imager	GOCI GOCI-II	Aerosols (SeaWiFS-like heritage)	2500 km rectangle, 8 images per day	2010+ Exp. 2018
	Second-generation spectral imager	AHI ABI AMI FCI	Aerosols and clouds (MODIS-like heritage products)	Fixed Earth disk centered above various longitudinal points, better than 30 minute scan repeat frequency	2015+ Exp. 2016 Exp. 2018 Exp. 2018
	UV/Visible-focused spectrometer	GEMS TEMPO UVNS	Mostly focused on trace gases (OMI-like heritage)	Fixed rectangle, scans roughly hourly	Exp. 2018 Exp. 2019 Exp. 2018
L-1	Spectral imager	EPIC/DSCOVR at the Lagrange-1 point	Aerosols, limited clouds (OMI-/SeaWiFS-like heritage)	Images whole sunlit portion of the Earth every ~90 minutes	2015+

interaction processes as illustrated in Fig. 2. Towards this end, recent large-scale international programs such as MILAGRO 2006 (Molina *et al.*, 2010) and GoAmazon 2014–2015 (Martin *et al.*, 2016), among other international campaigns, have been dedicated to perform air quality research involving heavy use of airborne platforms that offer mobility and flexibility. As reported by Lelieveld *et al.* (2015), Southeast Asia exhibits the second highest premature mortality rate, a large fraction of which is attributed to the trans-boundary air quality issues. Extensive aircraft operations in this region would undoubtedly be complex due to flight restrictions. Our *baseline* strategy for leapfrogging difficult trans-boundary (i.e., international) air quality research operations utilizes LEO/GEO satellites, dense ground-based network observations and regional-scale simulations, a grass-roots multi-country project whose conceptual layout is depicted in Fig. 3.

THE 7-SEAS/BASELInE CAMPAIGNS

Southeast Asia (SEA), an extensive agrarian region, has witnessed vibrant economic growth and rapid urbanization in recent decades. During boreal spring, biomass burning from natural forest fires and slash-and-burn agricultural practices strongly modulates the regional atmospheric composition over northern SEA. In the peak-burning season (March–April), aerosol species and associated trace gases degrade the regional air quality and impact the energy balance of the Earth-atmosphere system through their direct radiative effects. One of the most prevalent genres of clouds that modulate the radiative energy budget is the low-level stratocumulus (Sc) clouds (*cf.* Klein and Hartmann, 1993; Wielicki *et al.*, 2002; Hsu *et al.*, 2003; and references therein). These clouds cover more of the Earth's surface than any other cloud type, rendering them critical for distributing precipitable water in the Earth-atmosphere system as well as modulating the sensible and latent heat fluxes that profoundly affect weather and climate. Downwind from smoke source regions over SEA, the transported biomass-burning aerosols overlap and overlie a persistent low-level Sc cloud deck, associated with the development of the region's boreal spring cloud and rain system known as the *pre-Meiyu* (*cf.* Lau and Yang, 1997; and references therein). The onset and evolution of the South and East Asian summer monsoon systems (*cf.* Li *et al.* (2016) for a detailed review) may be influenced by the aerosol-cloud-precipitation interactions over Southeast Asia (e.g., Lee *et al.*, 2014) and remain active research topics. The low-level Sc clouds are particularly sensitive to changes in aerosol loading on both microphysical and macrophysical scales (*cf.* Wood, 2012; and references therein). Aerosols, by way of their size distribution and chemical composition, can trigger a plethora

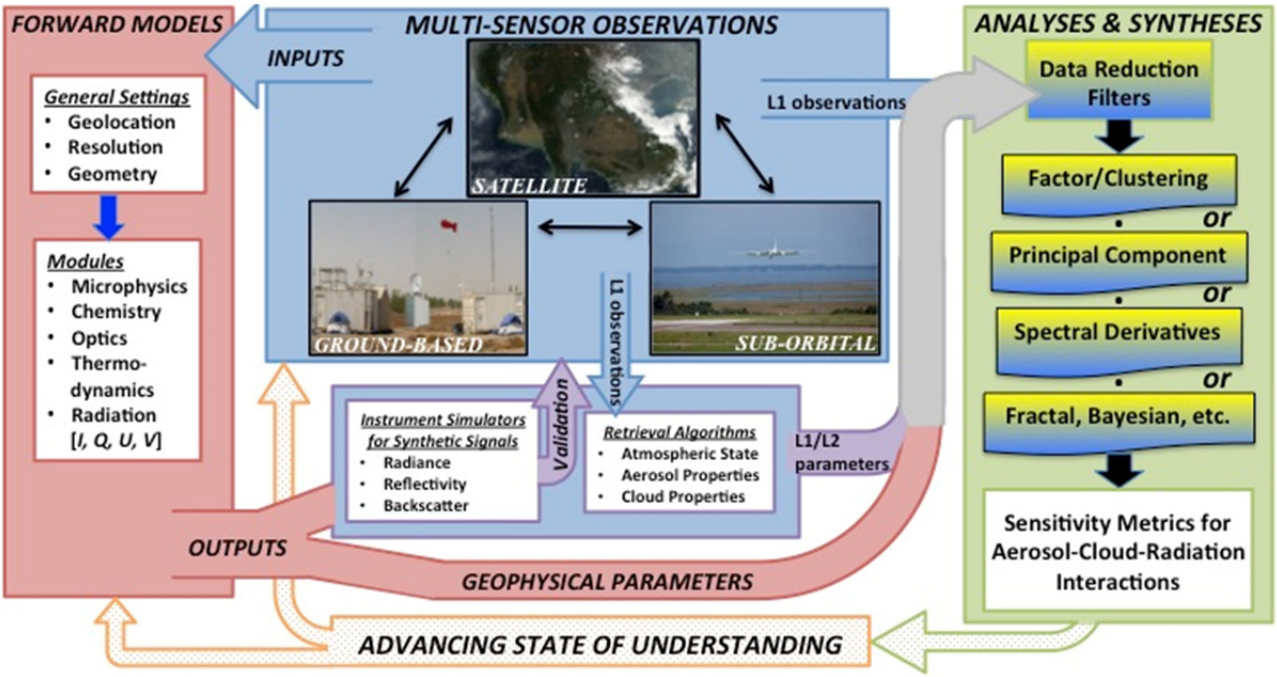

Fig. 2. Schematic of coordinated satellite, sub-orbital, and ground-based supersite/network, in conjunction with simulator/retrieval algorithms and analysis/synthesis modules advance the state of understanding of complex aerosol-cloud-radiation interaction processes. Snapshots of initial measurements (e.g., atmospheric state, aerosols, trace gases) provide 4-D (temporal + spatial) constraints to the forward models that drive instrument simulators to reproduce radiance/backscattering signals for assessing/validating cross-platform multi-sensor performance. The calibrated Level-1 (L1) spectral measurements together with forward-model products direct retrieval algorithms to generate a suite of L2 parameters (e.g., properties of gas/aerosol/cloud). Corresponding L1/L2 outputs from these sensors with geophysical parameters computed from the forward models are utilized in various analysis/synthesis approaches to develop sensitivity metrics that feedback for advancing the state of understanding in model simulations and observational strategies.

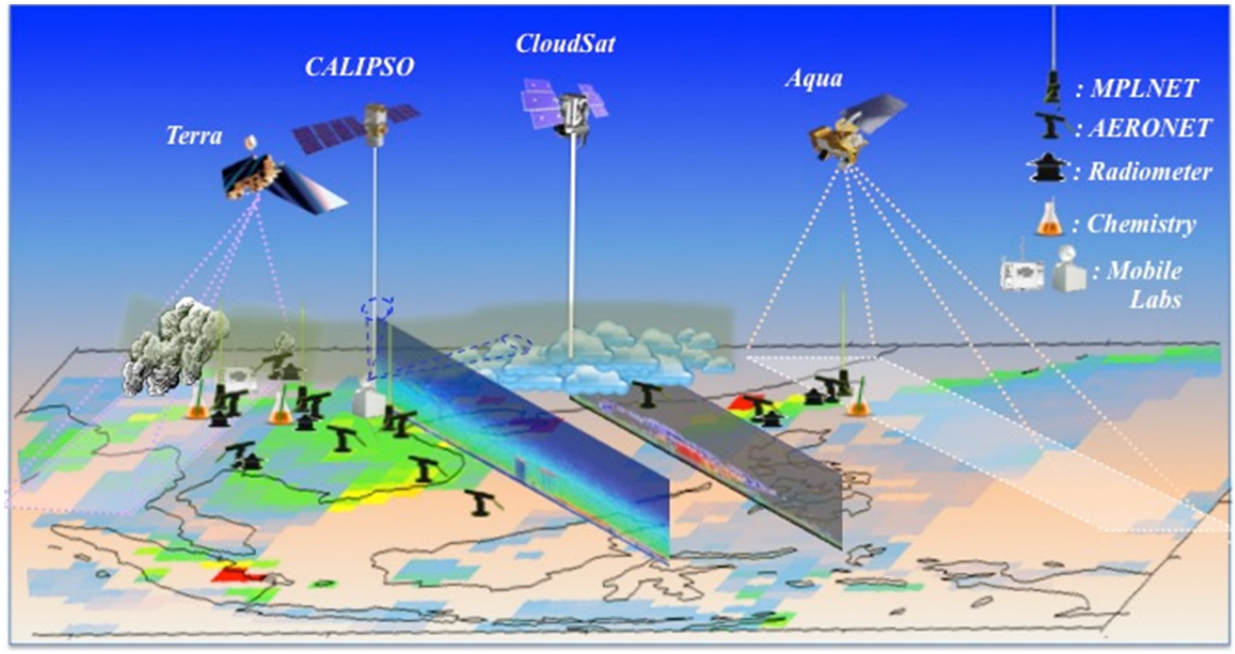

Fig. 3. Synergistic 7-SEAS/BASELInE deployments of AERONET/MPLNET, SMARTLabs mobile laboratories, and regional contributing instruments (all denoted by icons) along the "*river of smoke aerosols*" under various satellite overpasses to study the evolution of atmospheric composition due to springtime biomass-burning activities and complex aerosol-cloud-radiation interactions over land. Operational LEO satellites relevant to BASELInE campaigns were fully utilized. GEOs such as AHI/Himawari and EPIC/DSCOVR were not available during the IOPs of 2013–2015; they will be incorporated in the planning of future *BASELInE-like* IOPs. There are four supersites: near source regions at Doi Angkhang Met. Station, Thailand; long-range transport at Son La Met. Station, Vietnam; confluence of aerosols/clouds at Yen Bai Met. Station, Vietnam; and near sink areas at Lulin Atmospheric Background Station (LABS, ~2.8 km above sea level in the free-troposphere), Taiwan.

of reactions affecting the lifecycle of clouds. The aerosol-cloud system over SEA is *tightly* coupled and provides a unique, natural laboratory for further exploring the indirect radiative effects and complex interactions over micro- to macro-scales (*cf.* Lin *et al*., 2013; Reid *et al*., 2013; Tsay *et al*., 2013; Lin *et al*., 2014; and references therein). The nature and magnitudes of these complex effects are highly uncertain and remain poorly understood; most studies have focused mainly on marine environments, with far fewer studies over land where major sources of anthropogenic aerosols exist. The unique SEA climatology in boreal spring provides excellent atmospheric conditions (i.e., strong aerosol-cloud signals with dynamical processes not yet overwhelming the evolution of clouds, Tsay *et al*., 2013) to study the air quality and impacts of aerosols on Sc clouds and precipitation over land.

Reid *et al*. (2013) summarized extensively an interdisciplinary research program, 7-SEAS (Seven SouthEast Asian Studies), which focused mainly on the satellite aerosol remote sensing and associated observability issues over SEA, particularly the southern "Maritime Continent". To facilitate an improved understanding of the regional air quality as influenced by aerosol-cloud effects in climatologically important cloud regimes, *7-SEAS/BASELInE* (Biomass-burning Aerosols & Stratocumulus Environment: Lifecycles & Interactions Experiment) along with joint international efforts (i.e., regional contributing instruments) were conducted in spring 2013–2015 over northern SEA. Fig. 3 highlights a perspective of the region known as the "*river of smoke aerosols*" from near source regions over northern Thailand-Laos-Vietnam and depicts the confluence of aerosol-cloud-radiation interactions prior to entering the receptor areas of Hong Kong, Dongsha and Taiwan. The near-term research goals of 7-SEAS/BASELInE are: (1) to characterize the chemical, microphysical, and radiative properties of biomass-burning pollutants in the region, (2) to assess biomass-burning activities as they contribute to the regional air quality and meteorology, and (3) to evaluate how biomass-burning aerosols interact with seasonal Sc clouds. The success of these objectives constitutes building blocks from which the carbon, hydrological and biogeochemical cycles and radiative energy budget affecting the regional-to-global weather and climate can be further understood.

The experimental plan utilized to realize the research goals of 7-SEAS/BASELInE is illustrated in Fig. 3, which also summarizes the instrumental suites and their strategic locations. The general backbone of BASELInE observational network consists of AErosol RObotic NETwork (AERONET; Holben *et al*., 1998) sun-sky spectroradiometers and irradiance radiometers (Ji and Tsay, 2010; Ji *et al*., 2011), which can be deployed in a *DRAGON-like* (Distributed Regional Aerosol Gridded Observation Networks, Holben *et al*., 2016) configuration over a designated region to compare with airborne measurements and satellite retrievals or in a

Lagrange-like setting along prevalent pathways (Tsay *et al*., 2013) for the study of transport and evolution of the pollutants. To critically evaluate the latter, additional instrumentation is required. For this purpose, the supersites embedded in this setting include the SMARTLabs (Surface-based Mobile Atmospheric Research & Testbed Laboratories, *cf.* http://smartlabs.gsfc.nasa.gov) mobile facility, the MicroPulse Lidar NETwork (MPLNET; Welton *et al*., 2001, 2002), multi-suite of chemical samplers (Lin *et al*., 2013), and regional contributing instruments. Fig. 4 exhibits, for example, the ground-based instrumental layouts deployed during spring seasons in 2013–2015. In brief, SMARTLabs, AERONET, and MPLNET are comprised of suites of surface remote sensing and *in-situ* instruments that are pivotal in providing high spectral and temporal measurements, complementing the collocated observations from satellite platforms. Multiple suites of chemistry samplers (*cf.* http://aerosol.atm.ncu.edu.tw) deployed simultaneously over the region were used to quantify the composition of aerosols and precursors in considerable details to enhance our understanding of the air quality. Thus, 7-SEAS/BASELInE, the first of its kind in the region, is a collaborative effort between scientists from the U.S. (NASA, NRL, CSU) and from the region (Thailand, Vietnam, Hong Kong, and Taiwan). Building successful strategies and partnerships was an outcome of the mission that led many committed scientists nationally and internationally to tackle many aspects of satellite remote-sensing/retrieval and ground-based *in-situ* studies involving aerosols, clouds and air quality.

MEASUREMENTS AND PRODUCTS

In this section, we first present a typical example (*cf.* Fig. 5(a)) of extensive aerosols associated with biomass burning in relatively dry/cloud-free regions (i.e., northern Myanmar–Thailand–Laos) stretching hundreds of kilometers into cloudy areas (i.e., northern Vietnam, Hong Kong and southern China) during peak burning seasons in March–April. The MODIS/*e-DB* (*enhanced Deep-Blue*; Hsu *et al*., 2013) algorithm retrieved the full extent of smoke plumes from near-source to downwind cloudy regions, including aerosol optical thickness (AOT) above clouds (*cf.* Fig. 5(b)). This new above-cloud portion of the dataset (Sayer *et al*., 2016a) is currently operating on a case-study basis, and will be included in the MODIS Collection 7 data product suite. Measurements and retrievals of passive imagers are highly complementary to the information provided by active sensors (e.g., CALIOP/CALIPSO), offering wide swath coverage in contrast to the high vertical resolution (30 m) but limited "*curtain*" spatial coverage. Due to this curtain sampling, 9-year CALIOP backscatter profiles and feature mask data (Winker *et al*., 2009) from April 2007–2015 were analyzed to build a climatological picture of the vertical frequency distribution of aerosols and clouds in the region. Fig. 5(c), sampling over aerosol-cloud confluence area (blue-square box in Fig. 5(a), reveals a long-lived aerosol layer (red lines) peaking at ~3 km above sea level, while the occurrence of clouds (blue lines) ranges mainly between 2 and 3 km. Diurnal patterns, night time vs. daytime overpasses (dotted vs. solid lines in Fig. 5(c)), exhibit increases in the frequency of occurrence of both high- and low-level clouds and feature a deepening of the latter. The characteristic traits depicted resemble those of the near-source regions (brown-square box in Fig. 5(a), covering Doi Angkhang [DAK], Thailand, and Luang Namtha [LN], Laos) with the exception that the relative magnitudes of the aerosols and clouds are higher and lower, respectively. At low levels (e.g., below 3 km), often more than 50% of the lidar signals are totally attenuated (black lines in Fig. 5(c)) due to the widespread presence of aerosols and/or low clouds. In addition, this aerosol-cloud system is not only tightly coupled, but is also under active stratiform convection (Klein and Hartmann, 1993). Unlike deep convective clouds, complex dynamical forcing is generally absent in stratiform clouds, yet representing these clouds in climate models is challenging as the controlling processes (e.g., radiative cooling, turbulence, entrainment, precipitation) occur on relatively small scales, leading to uncertainties in future climate prediction (Wood, 2012).

The 7-SEAS/BASELInE integrated observational strategies take advantage of scheduled regional observations from space (*cf.* Table 1) and augmented/enriched by distributed network of ground-based measurements to fill in the missing gaps. Table 2 lists the durations of BASELInE operations and the locations of instrumentation deployed. Note that due to a large area to be covered, instrument availability and operational duration of each supersite may vary year by year with minor adjustments. Both AERONET's sun-sky spectroradiometer and MPLNET's vertical-pointing lidar with polarization capability are NASA's facility instruments and their instrumentation, measurement and processing are given in the links: http://aeronet.gsfc.nasa.gov and http://mplnet.gsfc.nasa.gov, respectively. Lee *et al*. (2016b), Sayer *et al*. (2016b), and Wang *et al*. (2015) have also utilized heavily the measurements of AERONET/MPLNET in this special issue. Lists of instruments hosted by SMARTLabs mobile laboratories can be found in Table 1 of Pantina *et al*. (2016, for *in-situ* probes) and Table 1 of Loftus *et al*. (2016, for remote sensing instruments). In addition, centralized command and data handling (C&DH) systems are implemented in SMARTLabs to provide a virtualized platform for a cohesive and consistent manner in which to interact with the independent instruments. The C&DH provides tremendous data storage, processing power, and communication interfaces (e.g., remote control/operation) to integrate the current instruments. These virtualization platforms provide great flexibility for deploying new or guest instruments without having to change the underlying support architecture, and increases reliability and decreases maintenance to allow SMARTLabs to perform in difficult environments with less manpower.

A compilation of chemistry samplers and other regional contributing instruments are listed in Table 3. As the sampling and analysis of atmospheric compositions are extremely laborious, chemical measurements in BASELInE campaigns were limited in duration to about six weeks in the intensive operating period (IOP). The samplers identified in Table 3 and their processing procedures are directed towards

Fig. 4. At the Doi Angkhang supersite, (a) panoramic view of all radiation instruments located at the highest point of the Met. Station water tower; (b) a simple shelter built on the floor underneath the water tower to host power supplies, dataloggers, computers and daily operations; (c) a suite of chemistry samplers from the Taiwan team were located on the platform next to SMART (2013), which hosted an MPLNET micro-pulse lidar, additional trace-gas and microphysics instruments with their inlets installed on the roof of SMART mobile laboratory; and (d) during 2014–2015 the micro-pulse lidar became a self-contained unit. At the Son La supersite, COMMIT (2012–2013) instrument setup for (e) AERONET sun-sky spectroradiometer; (f) GSFC irradiance radiometer set; (g) dual-channel (355 and 532 nm) lidar from Taiwan; (h) same as of (c), another suite of chemistry samplers from the Taiwan team; and (i) the COMMIT mobile laboratory. At the Yen Bai supersite, ACHIEVE (2013) instrument setup for (j) AERONET spectroradiometer with polarization for cloud-mode operations; (k) the ACHIEVE mobile laboratory in action; and (*l*) a 18.4 m high corner-cube (6.4-inch inner dimension) calibration tower, located on the west bank of the Red River, Vietnam, and 370 m from the ACHIEVE radars.

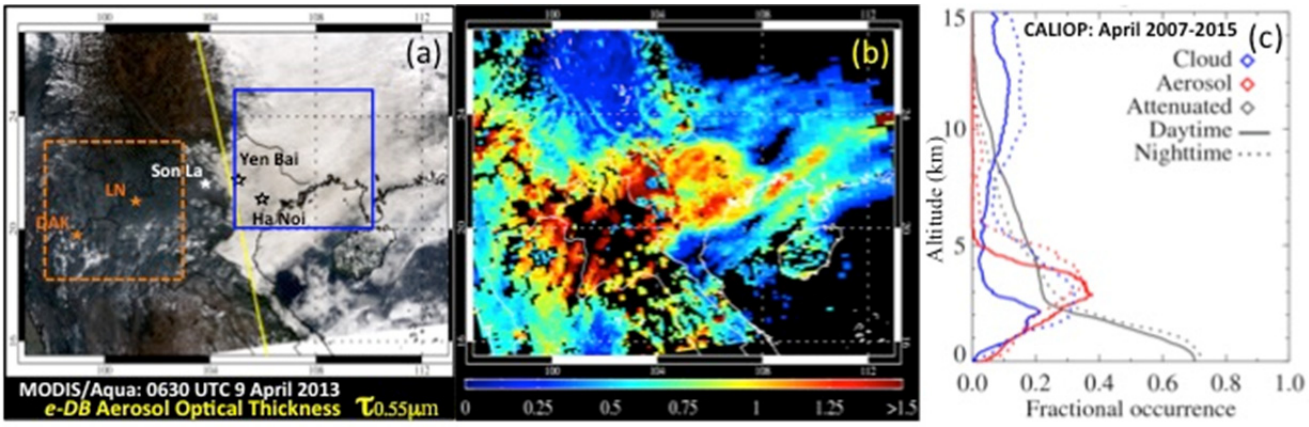

Fig. 5. (a) MODIS/Aqua red-green-blue image on 9 April 2013 covering the region of (16–27°N, 97–113°E) and the sub-regions of (20–25°N, 105–110°E, blue-square box)/(18–23°N, 98–103°E, brown-square box) superimposed with the A-Train overpass (yellow line) track over Southeast Asia, (b) the corresponding MODIS/*e-DB* AOT retrievals at 0.55 µm, and (c) CALIOP/CALIPSO aerosol and cloud vertical frequency distributions for April 2007-2015 day/night (solid/dotted lines, respectively) overpasses within the domain of blue-square box in (a).

Table 2. Locations (latitude, longitude, height above sea level) and duration (day/month/year) of 7-SEAS/BASELInE deployments along the *"river of smoke aerosols"*.

	Doi Angkhang (DAK)		Son La (SL)		Yen Bai (YB)		LABS		Others
	19.93°N, 99.05°E	~1.5 km	21.33°N, 103.90°E	~0.66 km	21.71°N, 104.87°E	~0.05 km	23.47°N, 120.87°E	~2.86 km	
AERONET	06/02–15/04/2013 26/02–14/04/2014 31/01–17/04/2015		14/03–09/04/2012 07/03–01/04/2013 04/03–15/07/2014 28/02–15/09/2015		31/01–09/04/2013		All year 2012–2015		[3]Cimel
MPLNET	05/02–15/04/2013 01/03–18/04/2014 15/03–18/04/2015		07/03–09/04/2012 21/02–07/04/2013 (Lidar from Taiwan)		–		All year 2013–2015 (at NCU campus)		–
SMART	06/02–16/04/2013		–		–		–		[4]SEBRA
COMMIT	01/02–13/04/2015		07/03–09/04/2012 21/02–07/04/2013		–		–		–
ACHIEVE	–		–		25/03–10/04/2013		–		–
Chemistry Sampler	06/03–08/04/2013 01/03–12/04/2014 01/03–13/04/2015		18/03–10/04/2011 13/03–19/04/2012 06/03–08/04/2013		–		06/03–08/04/2013 01/03–12/04/2014 01/03–13/04/2015		[5]HC
Others	[1]SU: Feb.–Apr. 2013 [2]CMU: 2013–2015		–		–		–		–

[1] SU: deployment of Silpakorn University's sensors: skyview 08/02–11/04/2013, Ground-based UV/PAR radiometer (GUV-2511) 12/02–11/04/2013, UV-Biometer & Luxmeter 13/02–29/03/2013.
[2] CMU: deployment of Chiang Mai University's Mini-Volume air samplers: 25/02–31/03/2013, 01/03–07/04/2014, 01/03–31/03/2015.
[3] Cimel: additional sites at Chiang Mai (Thailand), Maeson (foothill of DAK, Thailand, 2014), Luang Namtha (Laos), Ha Noi (Vietnam), Hong Kong, and Dongsha/NCU campus operated, covering the burning seasons in 2013–2015.
[4] SEBRA: Surface Energetics Broadband Radiometer Array deployed at additional sites during the burning seasons: Maeson (2014), Doi Angkhang (2013–2015), Luang Namtha (2013–2015, Laos), Son La (2012–2013), Hong Kong (2013), and Dongsha (2012–2013, Taiwan).
[5] HC: chemistry sampler package deployed at HengChun (Taiwan) site for the same duration as at DAK and LABS supersites.

determining the chemical composition (e.g., elemental/organic carbon [EC/OC], ions, volatile organic carbon [VOC], mercury, dioxin) and microphysical properties (e.g., size, mass, concentration) of the atmospheric aerosols and their precursors. Data products arising from the suites of ground-based measurements that are either remotely sensed or *in-situ* sampled are presented in Table 4. The two different kinds of products shown are those directly measured/retrieved (e.g.,

Table 3. Instruments, models, specifications (measurement types, size cuts), locations (2013–2015; or year-only), and manufacturer (Mfr.) for chemistry samplers operated in 7-SEAS/BASELInE.

	Instrument	Model	Specifications			Mfr.
			Measurement	Size Cut	Location (year-only)	
Standard	Honeycomb Denuder Particulate Sampler	RP-3500	Ions, BC, OC	PM_{10} & $PM_{2.5}$	DAK, LABS, SL (2013)	Thermo Scientific Inc., USA
	Particulate Sampler	PQ-200	Ions	$PM_{2.5}$	DAK, LABS, HC, SL (2013)	BGI Inc., USA
	High-Volume Air Samplers	PS-1	Dioxin, Metals, PAHs	Ambient & $PM_{2.5}$	DAK, LABS, HC, SL (2013)	Andersen Instruments Inc., USA
	High-Volume Air Sampler	HV-1000F	Dioxin, Metals	Ambient	DAK, LABS, SL (2013)	Sibata Scientific Technology Ltd., USA
Mission Specific	Mini-Volume Air Sampler	MiniVol™	Organics, SEM, FTIR	$PM_{2.5}$	DAK, SL (2013)	Airmetrics, USA
	Micro-Orifice Uniform Deposit Impactors	MOUDI-100/110	Aerosol size-segmented chemistry	Ambient	DAK, SL (2013), HC (2014–2015)	MSP Corp., USA
	Nano-Micro-Orifice Uniform Deposit Impactor	Nano-MOUDI-115	Aerosol size-segmented chemistry	Ambient	DAK (2013), SL (2013), HC (2014)	MSP Corp., USA
	High-Volume Air Sampler	Air Flow PM2.5HVS	Dioxin	$PM_{2.5}$	SL (2013)	Analitica Strumenti, Italy
	Mercury Ambient Sampler	MAS	Mercury (GEM, RGM, PHg)	Ambient	DAK, SL (2013), HC (2014–2015)	In-house, Taiwan
	Steam Jet Aerosol Collector	SJAC	Ions	$PM_{2.5}$	DAK (2013)	In-house, Taiwan
Regional	Mini-Volume Air Samplers	MiniVol	Ions, metals	$PM_{2.5}$	DAK	Airmetrics, USA
	Particle-Into-Liquid Sampler	PILS	Ions	$PM_{2.5}$	HC	In-house, Taiwan
	Flask Air Sampling	–	Greenhouse Gas	Ambient	HC (2015)	In-house, Taiwan

Note: BC/OC for black carbon and organic carbon, PAHs for polycyclic aromatic hydrocarbons, SEM for scanning electron microscope, FTIR for Fourier transform infrared spectroscopy, GEM for gaseous elemental mercury, RGM for reactive gaseous mercury, and PHg for particulate mercury.

spectral optical thickness, *in-situ* properties near surface) and those derived from combining products (e.g., aerosol hygroscopic growth factors). These products listed in the Table 4 reflect advances in methods of observations and technological progresses in instrumentation. As model simulations inevitably become more detailed (reflecting increased understanding of atmospheric processes), they will use and rely increasingly on such products and, as must be expected, will feedback new instrumental requirements and observational strategies. Indeed, such refinements have made possible predictive capabilities that describe how future changes in atmospheric composition affect climate and air quality. 7-SEAS/BASELInE measurements and data products set a *baseline* and are uniquely poised to address these challenges.

RESULTS

This paper provides an overview of new measurements/results from the 7-SEAS/BASELInE campaigns in 2013–2015. This volume is the third 7-SEAS special issue (after *Atmospheric Research,* vol. 122, 2013, which focused mainly on studies over the maritime continent; and *Atmospheric Environment,* vol. 78, 2013, whose purview encompassed measurements/analyses over northern SEA) and includes 27 published papers, which cover the following themes.

Regional Meteorology

The meteorological patterns over the Southeast Asian Peninsula (SAP) can be characterized by two distinct Asian monsoons: the winter northeast and the summer southwest monsoons (*cf.* Reid *et al*., 2013; Yen *et al*., 2013; and references therein). During the IOPs of 7-SEAS/BASELInE (2013–2015), the regional meteorology generally followed monsoonal wind fields, driven by the East Asian high and the westward expansion of the northwestern Pacific subtropical high. Biomass-burning smoke and associated air pollutants were prevalent in the boundary layer during the dry-winter monsoon season. In addition, during the peak-burning season of March–April, the local east-west cell/circulation, enhanced by a well-organized low-level convergent center over SAP, further uplifted the emitted pollutants into the

Table 4. Measurements and data products from SMARTLabs, AERONET/MPLNET, and regional contributing instruments, which include chemical composition samplers and other radiation sensors and *in-situ* probes.

SMARTLabs/AERONET/MPLNET	Regional Contributing Instrumentation
Aerosol Optics/Radiation: spectral optical thickness from UV to shortwave-IR, lidar extinction profile, and RGB scattering/absorption/extinction (*near surface*)	***Organic Carbon*** (OC): OC_1 (120°C), OC_2 (280°C), OC_3 (480°C), OC_4 (580°C), OP (pyrolyzed organic carbon), levoglucosan, dicarboxylic acids (oxalic acid, malonic acid, succinic acid, glutaric acid)
Aerosol Microphysics: mass, size-concentration, CCN, hygroscopic growth factor	***Elemental Carbon*** (EC): EC_1 (580°C–OP), EC_2 (740°C), EC_3 (840°C)
Cloud Optics/Radiation: zenith downwelling radiance (UV–μwave), linear depolarization, reflectivity profile	***Water soluble ions***: Na^+, NH_4^+, K^+, Mg^{2+}, Ca^{2+}, Cl^-, NO_3^-, SO_4^{2-}, nss-SO_4^{2-}, NO^{2-}, F^-, carboxylic acids
Cloud Microphysics: thermodynamic phase, water content, cloud-base/top/height, Doppler fall-velocity, particle size (in progress)	***Metals***: Al, Fe, Na, Mg, K, Ca, Sr, Ba, Ti, Mn, Co, Ni, Cu, Zn, Mo, Ag, Cd, Sn, Sb, Tl, Pb, V, Cr, As, Y, Se, Zr, Nb, Ge, Rb, Cs, Ga, La, Ce, Pr, Nd, Sm, Eu, Gd, etc.
Radiation Flux: solar and terrestrial irradiance	***Toxic***: Mercury, PCDD/Fs (dioxin)
Trace Gas – *Surface*: CO, CO_2, O_3, SO_2, NO_x/NO_y – *Column*: O_3, NO_2, SO_2, HCHO, CO, H_2O	***Aerosol Microphysics:*** mass ($PM_{2.5}$), particle morphology, filter-based particle absorption
Meteorology: P, T, RH, wind, mixed-layer height, precipitation, visibility	***Supplementary data:*** sounding profile, sky image, spectral UV (erythemal) irradiance

lower free-troposphere and transported them downwind to the east via westerly winds aloft (*cf.* Lin *et al*., 2013; Yen *et al*., 2013; and references therein). Furthermore, during the winter and spring months, low-level cloud layers consistently formed over the South China Sea/East Sea (SCS/ES) and Gulf of Tonkin. Drizzle from this cloud system frequently occurred over northern Vietnam from mid-winter into the pre-monsoon months (*cf.* Loftus *et al*., 2016; and references therein), yet it remains an understudied phenomenon relative to semi-permanent stratocumulus regions over the oceans (e.g., Klein and Hartmann, 1993; Tsay *et al*., 2013; Loftus *et al*., 2016).

Extending from the work of Yen *et al.* (2013), the NCEP/GFS (National Centers of Environmental Predication, Global Forecast System) analyzed data were used to study the nature of these clouds. Figs. 6(a)–6(c) demonstrate the mean large-scale circulation and specific humidity over SEA at three levels in the mid-to-lower troposphere during February–April for 7-SEAS/BASELInE. The area of anticyclonic flow at 700 hPa, straddling 15°N from the SAP to the northern Philippines (Fig. 6(a)), was associated with the sinking branch of a local Hadley cell (Klein and Hartmann, 1993). At 925 hPa (Fig. 6(c)), easterly and southerly flow rounding the base of the wintertime East Asian high advected moisture from SCS/ES over the SAP and southern China. Low-level convergent flow over the SAP induced upward vertical motion, maximized near 108°E, within the boundary layer beneath the subsidence region aloft, as evident from the mean induced vertical motion in the cross section along 22 °N for this period (Fig. 6(d)). In addition, the vertically integrated (surface to 700 hPa) water vapor flux depicts moisture convergence over the northern half of the SAP as evident by reductions in flux-vector lengths from south to north (Fig. 6(e)). This moisture convergence, combined with induced upward motion and capped by the upper-level tropical Southeast Asian high with blocking by mountainous terrain to the west, was conducive to the production and maintenance of low-level stratiform clouds over land.

Regionally abundant aerosols contribute to the modification of atmosphere-surface energy budget by modulating the radiative energetics. This is in addition to long-range transport and locally generated aerosols that heavily pollute stratocumulus clouds over land as well. The coupling of the microphysical influence of aerosols on cloud droplets affects cloud formation and lifetime, and may also impact precipitation processes. It is believed that decreasing trends in rainfall observed over the past 50+ years for this region (e.g., Phan *et al*., 2014; Schmidt-Thomé *et al*., 2015) may be partially attributable to increased aerosol loadings, particularly during boreal spring. The subsequent rainfall suppression may exacerbate the poor air quality conditions frequently observed over this region during the spring, making SEA uniquely valuable for analysis of aerosol-cloud-radiation interactions over land (*cf.* Loftus *et al*., 2016; and references therein).

Atmospheric Composition

Various aerosols and trace gases serve as efficient markers to distinguish the types and sources of biomass burning activities (*cf.* Andreae and Merlet, 2001; Kondo *et al*., 2011; Engling *et al*., 2013; and references therein). Several papers published in this special issue address physical and chemical properties of biomass-burning aerosols and trace gases from near-source regions over SEA to sink-receptor areas downwind, coordinated studies through *Lagrange-like* network approaches. Many datasets of trace gas (e.g., CO, CO_2, O_3, SO_2, and nitrogen oxides) measurements obtained from COMMIT at DAK (2015) and at SL (2012–2013) were analyzed and inter-compared to characterize the composition (and aging) of regional air masses, classified by meteorological episodes. Diagnostic ratios of tracer components (*cf.* Pantina *et al*., 2016; and references therein) yield characteristic signatures to aid in identifying different types of combustion (flaming or smoldering dominant) and source (biomass-burning or

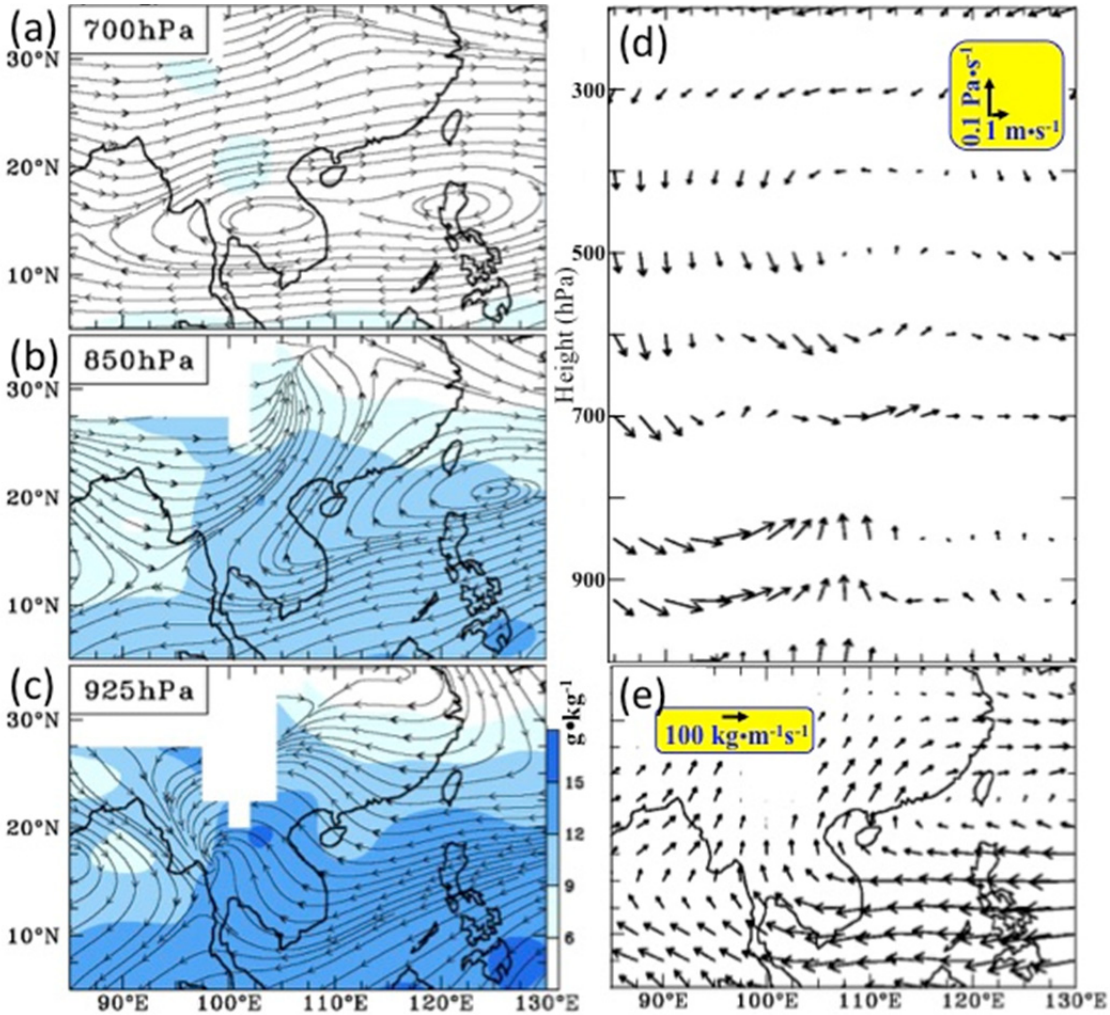

Fig. 6. During 7-SEAS/BASELInE of 2013–2015, (a–c) showing large-scale circulation over the SEA region, respectively, for the 700, 850 and 925 hPa pressure levels of February–April mean streamline and water vapor flux (in unit of g kg^{-1}); corresponding unit vector lengths, depicted in yellow boxes, for (d) mean induced vertical motion at the 22°N latitudinal cross section; and (e) water vapor flux integrated from surface to 700 hPa.

urban-pollution dominant). Sayer *et al*. (2016b) examined the temporal co-variability of aerosol and trace gas data recorded during the deployment. Peaks in biomass-burning aerosol concentrations (whether in terms of column AOT, surface PM-mass, or light extinction/absorption) and related trace gases showed the same distinctive patterns throughout the IOP. This was also true to an extent in terms of diurnal variability: within an individual day, expansion of the planetary boundary layer in the local late morning brought increases in both aerosol levels and CO_2 at the DAK site. Furthermore, adding radon measurements as an additional trace gas proxy of atmospheric transport and mixing processes, Chamber *et al*. (2016) demonstrated an improved method for representing trans-boundary transport of anthropogenic pollution in East Asia. Chen *et al*. (2016) also presented correlation analyses of total gaseous mercury and the aforementioned trace gas pollutants (including PMs) to distinguish the climatic characteristics (e.g., scenario vs. background mercury) of the measurements and to determine their discriminating factors.

Aerosol morphology (e.g., size, shape), composition (e.g., organic/inorganic) and surface functionalities (e.g., hydroxyls, carbonates, and sulfates) are invaluable for constructing improved aerosol models used in optical closure and energy budget studies (e.g., Bell *et al*., 2013). Various size-cut inlets (ambient, PM_{10}, $PM_{2.5}$, PM_1) and filter samples (e.g., Teflon, Quartz) were collected at near-source (DAK), transport-pathway (SL) and sink-receptor (LABS and HC) sites. In addition, quartz filter analyses for separating OC and EC are routinely performed in BASELInE IOPs. Lee *et al*. (2016a) thoroughly investigated various chemical species and their distinctive concentration gradients in $PM_{2.5}$ at SL site in spring 2012–2013. Carbonaceous (OC and EC) matter constituted the major portion of the fine PM mass burden in the biomass-burning regions, in contrast to typical observations in urban areas, which are primarily comprised of sulfates. OC3 (evolution temperature at 280–480°C) and EC1-OP (elemental carbon evolved at 580°C minus the pyrolized OC fractions) were the most abundant OC and EC fractions, respectively. Water-soluble

inorganic ions (SO_4^{2-} and NH_4^+) varied widely and indicated the influence of trajectory paths with anthropogenic origins. K^+, OC3, EC1-OP, and levoglucosan were also analyzed and found as valuable tracers of biomass-burning activities. Moreover, Popovicheva *et al*. (2016) categorized a wide range of observed $PM_{2.5}$ mass concentrations from low to high smoke intensity during the IOPs at SL, significantly departing from the WHO (World Health Organization) air quality standards. Using a variety of techniques (e.g., Scanning Electron Microscopy-Energy Dispersive Spectroscopy, Fourier Transform Infrared Spectroscopy, Hierarchical Cluster Analysis), the analyses of carbon fractions, organic/inorganic functionalities, and individual particle grouping lead to the conclusion that ambient aerosols at SL are highly affected by emissions from the smoldering combustion of wood and other local biomass species.

Stable carbon isotopes in these aerosols can be helpful in understanding the sources of aerosol organic carbon (e.g., Turekian *et al*., 2003; Fu *et al*., 2012; Wozniak *et al*., 2012). Nguyen *et al*. (2016) comprehensively investigated the $PM_{2.5}$ organic molecular composition and stable carbon isotope ratios of biomass-burning smoke for the first time at SL site, by using gas chromatography-mass spectrometry (GC-MS). Fourteen representative $PM_{2.5}$ samples were collected in spring of 2013 and analyzed for more than 50 organic compounds including primary (i.e., anhydrosugars, lignin and resin products, sugars, sugar alcohols, fatty acids, and phthalate esters) and secondary (i.e., aromatic acids, polyacids, and biogenic oxidation products, such as 2-methyltetrols, alkenes triols, and 3-hydroxyglutaric acid) organic aerosol components. The selected samples were comprised of mixtures of burned softwood, hardwood, grass, and non-woody vegetation. Levoglucosan was found as the predominant (comprising 2.23 ± 0.5% of $PM_{2.5}$ mass) species among aerosol sugars. Backward trajectories of the sampled air masses suggested strong influence of biomass-burning aerosols originating from the SAP compared to the relatively lower impact from urban or industrial origins in southern China and the maritime SCS/ES.

Khamkaew *et al*. (2016) investigated the elemental and ion composition of biomass-burning aerosols obtained from near-source (DAK) and urban (CM; Chiang Mai, Thailand, ~200 km south of DAK) sites during the 2014 BASELInE IOP. Enriched tracers from K^+, NO_3^- and levoglucosan confirmed the major influence of biomass-burning activities, and the principal component analysis revealed that agricultural activities, soil re-suspension and road traffic were the additional sources of $PM_{2.5}$ over the sites. Furthermore, Wiriya *et al*. (2016) thoroughly investigated and analyzed the emission factors of PM_{10} and polycyclic aromatic hydrocarbons (PAHs) from the burning of leaf litter, maize residue and rice straw in a stainless steel chamber at CM site. They concluded that the burning of forest leaf litter emitted higher amounts of particulate pollutants than the agricultural residue burning. In turn, the emission rates of pollutants from forest burning were found to be much higher than those from agricultural field burning, mainly due to larger burnt areas in the forest. Moreover, this study also provides insights and essential information to policy makers involved with regulatory actions in air quality management in the northern part of Thailand.

$PM_{2.5}$ can be transported a long distance to the downwind area. Fujii *et al*. (2016) collected $PM_{2.5}$ at Bangi (~25 km south of Kuala Lumpur), Malaysia, in September 2013, and derived that organic matter was the most abundant component in $PM_{2.5}$ mass followed by non-sea-salt sulfate and EC. They also found that biomass burning was the main contributor to ambient EC concentrations compared to coal combustion and motor vehicle emissions during the southwest monsoon season. Similarly, Kim Oanh *et al*. (2016) characterized both $PM_{2.5}$ and $PM_{10-2.5}$ at Khao Yai National Park (700 m above sea level and 120 km upwind to Bangkok) in Thailand, during the dry season. Secondary particles and their gaseous precursors transported from distant sources to the site were shown to be more important contributing factors to $PM_{2.5}$ levels. In contrast, most of the contributors to $PM_{10-2.5}$ could be linked to local sources except for the sea spray, which would be linked to a distant source origin. Oozeer *et al*. (2016) performed WRF-Chem simulations to identify the cause of the intensification of the transport of biomass-burning emissions from Sumatra to Peninsular Malaysia under deep convection weather conditions, which uplift these pollutants to the upper troposphere, potentially influencing the global climate via significant long-range transport. Furthermore, Chuang *et al*. (2016b) used the CMAQ (Community Multi-scale Air Quality) model to exploit the chemical evolution during the long- (short-) range transport of biomass-burning (anthropogenic) aerosols from SEA to LABS. This study revealed that the high-altitude biomass-burning aerosols influence the air quality on the ground through mechanisms of (1) subsidence in anticyclone, (2) mixing in the boundary layer, and (3) downward flow in the cold surge from Asia.

Remote Sensing of Air Quality and Impact on Radiative Energetics

The optical (e.g., spectral blue-green-red scattering/extinction, ultraviolet to near-infrared absorption) and microphysical (e.g., number, mass, dry/wet size distribution) properties of aerosols play vital roles in influencing regional air quality; these were measured with identical instrument sets at the BASELInE supersites (i.e., DAK, SL, and LABS), along with distributed AERONET retrievals of columnar AOT and other aerosol properties. Although PM concentration is most accurately measured using ground-based devices, the sparsity of their areal coverage precludes use of such measurements solely to determine local and regional variation of PM. The use of satellites for monitoring surface PM levels is an attractive possibility, due to their broad spatial coverage. However, as passive satellite sensors are in general sensitive only to the columnar aerosol optical properties, as opposed to the desired quantity of surface-level mass, the task is not straightforward (e.g., Hoff and Christopher, 2009; Paciorek and Liu, 2009).

Many factors can affect the relationship between columnar AOT retrieved by satellites and surface PM-mass concentrations. Typical approaches tend to use some form

of empirical regional/seasonal tuning or chemistry transport model to represent the link between optical and mass loading, as well as meteorological data to account for quantities such as PBL (planetary boundary layer) height or humidity (e.g., van Donkelaar *et al*., 2010, 2014; Wang *et al*., 2014). The former particularly plays an important control, as for a constant aerosol loading, on diurnal expansion and contraction of the PBLH (PBL height) decreases and increases respectively the surface-level aerosol loading, which can be significant in much of SEA. Wang *et al.* (2015) investigated aerosol columnar properties and vertical distributions using AERONET/MPLNET measurements and surface data of $PM_{2.5}$ mass concentration from local air quality stations during BASELInE campaigns. Consistent spatiotemporal patterns were found between AERONET/AOT, satellite retrieved AOT, and local PM/mass, suggesting the presence of widespread smoke aerosols that influence air quality over the region. Moreover, MPLNET lidar profiles further illustrated aerosol diurnal variability strongly dominated by the PBL dynamics, with aerosol mixed-layer height extending from the surface to 5 km above sea level. As the smoke particles ascend (normally in late afternoon), they have a high potential for long-range transport by the westerlies and influence the air quality downwind. In addition, Sayer *et al.* (2016b) presented a satellite/surface perspective on biomass burning from observations near source regions at DAK, which sampled a mixture of local burning and smoke transported from Myanmar to the west. Space-based (MODIS) and ground-based (AERONET) columnar AOT also showed strong diurnal variability, even in the small 3-hour window between the Terra and Aqua satellite overpass times. This variability was linked to the strong diurnal cycle of PBLH, which proved to be the main controlling factor in the ratio of column AOT to surface PM mass throughout the day. Although hygroscopic growth effects were observed (Pantina *et al*., 2016), these were secondary in terms of effect on the AOT/PM-mass ratio in BASELInE IOPs.

Likewise, over the maritime continent, Chew *et al*. (2016) studied the regional aerosol environment in Singapore and showed an improved relationship between $PM_{2.5}$ concentration and AOT, normalized by MPLNET-derived scale height. Based on nighttime Raman lidar measurements in Penang Island, for the first time in Malaysia, Hee *et al*. (2016) were able to identify the presence of marine/urban aerosols in the background, irrespective of monsoon seasons, even though wood burning and aged forest fire aerosols prevailed during biomass-burning episodes. Kusumaningtyas *et al*. (2016) reported for the first time that an exceptionally high value (~6) of AERONET/AOT due to peatland fire was observed in 2012–2014 at the Central Kalimantan site (Indonesia), where a high mean-value of single-scattering-albedo (SSA, ~0.94) also indicates a clear signature of underground smoldering. Furthermore, Qi *et al*. (2016) reported that aerosol optical properties exhibited high value in absorption AOT and high aerosol volumes, low SSA in coarse mode after agricultural burning of rice straw in East China.

Lee *et al.* (2016b) applied ASHE (Aerosol Single-scattering-albedo and Height Estimation) satellite algorithm to produce a large-scale spatial distribution of the heights of biomass-burning aerosols over SEA. Utilizing measurements of AERONET (e.g., spectral AOT, SSA) and MPLNET (e.g., extinction profile) during BASELInE IOPs, ASHE products were examined (and uncertainties estimated) extensively in particular over areas outside the CALIOP track, which had not been available using CALIOP measurements only. The implications of ASHE products (particularly from GEO satellites) can provide diurnal cycle of the height of biomass-burning aerosols in the region, which are critical in advancing our understanding and assessment the impact of the biomass-burning aerosols on air quality.

Biomass-burning aerosols are significant contributors to the regional/global aerosol loading and to the modulation of surface-atmosphere radiative energetics during their lifecycles (e.g., Crutzen and Andreae, 1990; Penner *et al*., 1992). Extending from the optical closure modeling (Bell *et al*., 2013; Pani *et al*., 2016a) for regional biomass-burning aerosols, Pani *et al*. (2016b) reported, for the first time, a detailed estimation of direct aerosol radiative effect (DARE) near source regions over northern SAP by using *in-situ* datasets (i.e., ground-based measurement of aerosol physical, chemical, and optical properties) and a radiative transfer model during the spring of 2013 BASELInE campaign. Their results provided strong evidence that biomass-burning aerosols (mainly water soluble and black carbon) enhance the surface cooling (as high as –33.5 W m^{-2} in 24-hour mean) as well as atmospheric warming (as high as +24.7 W m^{-2}), which could significantly influence the diurnally-averaged radiative energetics. Moreover, the contribution of solely black carbon aerosols towards the atmospheric warming was up to 75% near source regions. Whereas the variability of aerosol composition affects regional radiative energetics, Gautam *et al*. (2013) also showed the aerosol vertical distributions, in terms of diurnal cycle, could be an important factor on influencing DARE.

Arola *et al*. (2013) used AERONET data to investigate the extent to which the diurnal cycle of the DARE could be estimated without knowing the diurnal cycle of AOT. Taking the diurnally-resolved AOT as the *ground-truth* from which to assess the approximation errors, comparisons were performed of the DARE calculated from the daily-mean AOT, as well as those evaluated near the Terra/Aqua overpass times. While the global-average effect on calculations was fairly small, Arola *et al*. (2013) concluded that not knowing the AOT diurnal cycle could cause significant uncertainty in DARE estimates on a regional and seasonal basis. For example, at one site (Silpakorn University, Thailand at 13°N, 100°E) in SEA spotlighted in the study, during the springtime biomass-burning season, only observing at the Terra (10:30 am) or Aqua (1:30 pm) overpass led to a mean error in the calculated DARE of +0.49 and –0.19 W m^{-2} respectively, compared to that calculated from the full AOT diurnal cycle. Other regions in SEA more strongly influenced by biomass burning are likely to be even more greatly affected. These results underscore the importance of observations of the diurnal cycle of aerosol loading in complex regimes such as those occurring at SEA. Analyses of ground-based irradiance measurements and collocated

AERONET/AOT along aerosol-laden regions (e.g., DAK-LN-SL) during BASELInE IOPs are currently underway.

Hygroscopicity and Aerosol-Cloud-Radiation Interaction

The interactions among aerosols, clouds, and radiation can be categorized into first-order and higher-order processes: the former represents light-absorbing aerosols and clouds co-existing *interstitially* (or decoupled) to modulate the radiation fields in the combined system; the latter is rooted in the role of aerosols serving as cloud-condensation-/ice-nuclei (CCN/IN). Complex cloud feedbacks (e.g., fraction, lifetime) from the CCN/IN activation can influence accurate quantifications of energetic and hydrological budgets of the aerosol-cloud system, which remain the largest uncertainty in climate-related studies (*cf.* IPCC, 2013; and references therein). The ability of atmospheric aerosols to uptake water (i.e., their hygroscopic behavior) and become CCN may occur at ambient relative humidities (RHs) well below supersaturation. Moreover, hygroscopicity can modify the physical properties of aerosols (e.g., size, density, mass) as well as their lifetime.

Pantina *et al.* (2016) demonstrated the COMMIT dual-system scheme to exploit aerosol hygroscopicity through measurements of inter-correlated properties: light scattering (by RH-adjustable wet/dry Nephelometers), particle size (by wet/dry Scanning Mobility Particle Sizers, or SMPS), and activation (by CCN counter with pre-set supersaturation levels). The aerosol dynamical processes (e.g., coagulation, condensation, deposition), optical properties (e.g., light scattering/absorption) and interactions with clouds and radiation (and/or precipitation), all depend on their size to first-order, and secondly on their chemical composition (Dusek *et al.*, 2006). The hygroscopicity of particles alters not only their light scattering properties by changing their size and refractive index (*cf.* Brem *et al.*, 2012; and references therein), but also greatly increases the light absorption by BC aerosol internally mixed with hygroscopic materials through radiation lensing effects (e.g., Redemann *et al.*, 2001). To a lesser extent, the absorbed water for hygroscopic aerosols could provide a medium for heterogeneous chemical reactions in the atmosphere (Khlystov *et al.*, 2005) and also changes the partitioning of semi-volatile species between the gas and aerosol phase (Ansari and Pandis, 2000). In addition, water uptake of aerosols is a key factor influencing their growth in size and deposition inside the humid respiratory tract and exact corresponding health effects (Löndahl *et al.*, 2009; Engelhart *et al.*, 2012; Martonen *et al.*, 2003). Thus, one compelling reason for using *in-situ* measurements to fully study the aerosol hygroscopicity is that none of the current operational satellite algorithms retrieve hygroscopic properties of ambient aerosols; however, these properties have been identified by modeling studies as a significant source of uncertainty when predicting their influences on air quality and radiative forcing on regional-to-global scales (e.g., Wang and Martin, 2007; Achtert *et al.*, 2009; Pekour *et al.*, 2012; Titos *et al.*, 2014).

Petters and Kreidenweis (2007) derived a one-parameter model, the so-called κ-Köhler theory, where the hygroscopicity parameter (κ) represents a quantitative measure of aerosol water uptake characteristics and CCN activity. The κ-parameter also can be derived from hygroscopic growth factor measurements such as wet/dry SMPS/H-TDMA (hygroscopicity-tandem differential mobility analyser) size distributions (e.g., Carrico *et al.*, 2010) and wet/dry nephelometer scattering data (e.g., Jeong *et al.*, 2007; Zieger *et al.*, 2013). These approaches provide useful metrics for constraining the CCN activity in, for example, cloud-resolving models, which may help clarify the connections between aerosol hygroscopicity and cloud-radiation-precipitation interactions. During the 2013 BASELInE campaign at DAK, Hsiao *et al.* (2016) reported that the values of κ-parameter were low (0.05–0.1) and correlate well with the amount of particulate organic matter. These observations were comparable with those of κ-parameter estimated from H-TDMA measurements (κ ~0.07–0.08) in the Amazonia (Rissler *et al.*, 2004, 2006), as well as consistent with previous studies on water uptake of carbon-dominated aerosols (e.g., Petters *et al.*, 2009; Carrico *et al.*, 2010; Dusek *et al.*, 2011; Engelhart *et al.*, 2012). Although κ-values derived from ground-based observations of biomass-burning aerosols are generally less than 0.1, with sufficient atmospheric updraft velocity (i.e., strong adiabatic cooling) the aerosols can serve as CCN and influence cloud microphysical and radiative properties (e.g., West *et al.*, 2014). Reutter *et al.* (2009) have further investigated the sensitivity of the formation of cloud droplets to κ-values under pyro-convective conditions and found that a 50% change in κ alters the droplet concentration by more than 10% for aerosols with very low hygroscopicity ($\kappa < 0.05$) in the updraft-limited regime. Thus, biomass-burning aerosols in northern SEA could fall in the updraft-sensitive regime (transitional, Reutter *et al.*, 2009) and the formation of cloud droplets depends nonlinearly on both CCN concentration and updraft velocity. This highlights the importance of hygroscopicity and aerosol-cloud-radiation interactions over SEA.

Loftus *et al.* (2016) introduced the first ground-based W-band radar (94 GHz) observations of the semi-persistent springtime low-level stratocumulus cloud layers over northern Vietnam during the 2013 BASELInE campaign, and the applications of these measurements to modeling aerosol-cloud-radiation interactions. As these cloud systems often impinge upon the plume of biomass-burning aerosols over the region, observing the cloud lifecycles is a key step to assessing potential feedbacks within the coupled cloud-aerosol system, as well as the impacts of these feedbacks on local and regional air quality. Preliminary cloud model simulations based on the observations reveal drizzle suppression is likely as the atmospheric aerosol burden increases. This may exacerbate the issue of poor air quality over the region during the pre-monsoon months as precipitation processes can have a large role in removing aerosol particles from the atmosphere. Improved representation of aerosol, cloud, and precipitation processes in models, along with comprehensive collocated and network observations of aerosol and cloud properties, will greatly benefit our understanding not only on the meteorological impacts of biomass-burning aerosols, but on human health as well.

Air Quality and Implications to Health

Air pollution has been classified as a potential source of carcinogens and other toxins hazardous to humans (Group 1) by the International Agency for Research on Cancer (IARC). In 2010, air pollution resulted in 3.2 million premature deaths worldwide mainly due to cardiovascular disease and 223,000 deaths from lung cancer (Lim *et al*., 2012; IARC, 2013). Biomass-burning smoke and associated air pollutants typically reach a peak level during the pre-monsoon season in SEA and biomass burning has been related to the development of chronic obstructive pulmonary disease (Idolor *et al.*, 2011). However, the emissions over SEA have garnered less attention than those in other tropical regions (Lin *et al*., 2013, 2014). Biomass-burning activities significantly contribute to regional pollutant emissions (Carmichael *et al*., 2009; Tsay *et al*., 2013; Chang *et al*., 2015). The resultant poor air quality and haze episodes cause significant pollution levels, such as PM, that far exceed regional air quality standards (Chew and Bhatia, 2008; Lyu *et al*., 2015). Lee *et al.* (2016a) showed that average $PM_{2.5}$ mass concentrations were approximately 51–57 μg m^{-3} in northern Vietnam, which was approximately 2-fold higher than the WHO $PM_{2.5}$ guideline (25 μg m^{-3} 24-h mean). Seasonal emission has been recognized as an important issue, the peak of which occurs prior to the onset of the summer monsoon rains and is prevalent over forested regions (Fujii *et al*., 2016). Consistent results indicated that biomass-burning activities are critical emission sources for air pollutants such as $PM_{2.5}$ in SEA, which may lead to adverse health effects. However, the effects of local air pollution on human health in SEA remain unclear.

The lung is the main portal of entry for particulate and gaseous pollutants and as such, a critical organ for whole body defense, by the clearance of deposited foreign materials. Most of the diseases associated with exposure to air pollution are initiated within the respiratory-to-cardiovascular system. Seaton *et al*. (1995) demonstrated that particles deposited in the lung environment provoked a low-grade alveolar inflammation with a secondary systemic inflammation. The potential toxicity of inhaled foreign materials in the vapor phase, liquid droplets and solid particles are dependent upon the interaction with the respiratory system. The extent to which particle deposit and remain in the airway is a function of the flow rate, penetration and clearance mechanisms (Squadrito *et al*., 2001). Particle size is usually categorized according to its ability to penetrate the respiratory system. Thoracic particles (particle of < 10 μm in aerodynamic diameter, PM_{10}) can readily penetrate and deposit in the tracheobronchial tree (BéruBé *et al*., 2007), whereas fine particles ($PM_{2.5}$) bypass the upper airways and are deposited in the lower and distal lung environments (Bai *et al*., 2001; Monn *et al*., 2003). A considerable amount of research has been devoted to ultrafine particle (or nanoparticles) that can be inhaled into the alveolar region due to their unique size-range fraction. Hata *et al*. (2014) indicated that more than 30% of combustion-derived particles from the burning of biomass had a mass that fell within a size range of < 100 nm. Notably, Chuang *et al*. (2016a) observed that high concentrations of nanoparticle surface area (100.5 ± 54.6 $\mu m^2\ cm^{-3}$) emitted from biomass burning in SEA can be inhaled into the human alveolar region. Additionally, these alveolar-deposited biomass-burning nanoparticles are associated with fires burning at different locations within a radius of 100–150 km from DAK, where most people live. The findings suggested that the quality of people's lives in this region could be compromised by the presence of biomass-burning particles that may be deposited in the lungs. In susceptible groups, these particles are more likely to remain in the alveolar regions for longer times due to air trapping, leading to elevated particle toxicity (Hazucha *et al*., 2013; Patterson *et al*., 2014).

Reactions by humans to compound-specific toxic particles are essential issues that must be considered. PAHs, nitro-PAHs and metals, for example, are the predominant constituents in biomass-burning $PM_{2.5}$ (Chuesaard *et al*., 2014; Tian *et al*., 2014) and are recognized toxic agents (Chuang *et al*., 2012). Likewise, burning of forest and backyard open-trash become important sources of polychlorinated-p-dibenzo dioxin and dibenzofurans (PCDD/Fs) and dioxin-like compounds, formed during combustion processes in the presence of chlorine and catalysts (e.g., copper, iron). Chang *et al.* (2014) reported during rice straw burning periods PCDD/Fs and polybrominated diphenyl ethers (PBDEs) concentrations in the atmosphere measured near the farm site increased dramatically by six to twenty times. However, Pongpiachan (2016) concluded that $PM_{2.5}$-bound PAHs did not increase significantly the risk of cancer in northern Thailand between biomass-burning and non-biomass-burning seasons. Their results may be argued on the basis of the insignificant increases of PAH concentrations during biomass-burning seasons relative to the background pollutants (e.g., traffic emissions) from human habitations. Chang *et al.* (2013) and Chi *et al.* (2016) hypothesized that the increased levels of dioxin and dioxin-like compounds measured at LABS were contributed by the biomass burning in northern SAP and under favorable long-range transport conditions. Nguyen *et al*. (2016) observed 50 organic compounds present in biomass-burning particles. For example, sugar and sugar alcohol compounds, fatty acids, phthalate esters, aromatic acids, poly-acids and biogenic oxidation products were identified in biomass-burning $PM_{2.5}$; their potential as health hazards is the subject of a future study. In addition, Gupta *et al*. (2016) studied the effects of dustfall deposition on foilar surfaces of two medicinally important plant species. In terms of surface morphology and biochemical constituents, it was found that dust deposition caused adverse effects on the foliar surface, cuticle and epidermal layers.

To summarize, biomass-burning smoke contains significant amounts of nanoparticles whose surface area provides a substrate for reactions with chemicals such as PAHs (Sevimoglu and Rogge, 2015; Tiwari *et al*., 2015). This implies that particles emitted from biomass-burning activities may have a greater potential of inducing oxidative-inflammatory responses and carcinogenesis in the lungs (or other tissues) after inhalation. The unique techniques employed in 7-SEAS/BASELInE advance the understanding of human health as it is affected by biomass burning from macro- (satellites) to micro-environment (cellular

mechanisms). A time-series investigation of particle toxicity in SEA can provide more information for risk assessment and human health protection as well as furthering our understanding of the modification of toxins during aerosol/cloud formation and transport.

SUMMARY AND FUTURE WORK

In this overview paper, we present an integrative summary on the concept/deployment of 7-SEAS/BASELInE campaigns with highlights of papers published in this special issue, emphasizing air quality and aerosol-cloud effects on the environment. These papers represent the second wave of analyses using 7-SEAS/IOPs' measurements and serve as an anchor point for future studies and deployments in northern SEA for advancing our state of understanding of the complex aerosol-cloud-radiation interaction processes. All 7-SEAS/BASELInE measurements and data products are open to the public and any research communities. AERONET and MPLNET data are available respectively from http://aeronet.gsfc.nasa.gov and http://mplnet.gsfc.nasa/gov. The SMARTLabs website is http://smartlabs.gsfc.nasa.gov and data can be requested from S.-C. Tsay. Measurements and data products from regional contributing instruments (http://aerosol.atm.ncu.edu.tw/7seas) can be requested from N.-H. Lin.

Through the use of current measurements and data products from 7-SEAS campaigns and model simulations, we envision that future *BASELInE-like* measurement/modeling needs fall into two categories: (1) efficient yet critical *in-situ* profiling (e.g., tethered ballroom, Unmanned Aerial Vehicle) of the PBL for validating remote-sensing/retrievals and for initializing regional transport/chemical and cloud ensemble models, and (2) fully utilizing the high observing frequencies of satellites (e.g., GEO, L1; *cf.* Table 1) for resolving the diurnal cycle of PBLH, furthering our understanding as to how it affects biomass-burning aerosols that play such a crucial role in air quality and in radiative energetics. Representing the controlling processes (e.g., radiative cooling, turbulence, entrainment, precipitation) of stratiform clouds in the aforementioned models is challenging. Complexity is exacerbated by the fact that aerosol-cloud-radiation (-precipitation) interaction processes are highly dependent on the state of the atmosphere characterized by its stability, humidity, composition of soluble gas species present that facilitate droplet nucleation as well as the properties of ambient aerosol types (e.g., hygroscopicity). Thus, *in-situ* profiling of the PBL at optimal temporal and spatial resolutions are critically needed for validating retrievals from collocated remote sensing instruments (e.g., spectrometer, interferometer, lidar, radar) and for initializing the controlling processes (e.g., amount, type, distribution of atmospheric constituents) in the regional transport/chemical and cloud ensemble models.

Nearly continuous observations from the surface enable a more detailed understanding of the lifecycle of meteorological processes, not otherwise possible from space-borne platforms, mitigating spectral/temporal issues associated with spatial sampling. Hence, surface observations at the regional scale complement satellite observations at the global scale. Furthermore, wide excursions in aerosol loading and meteorological parameters over SEA associated with diurnal variability reveal a fundamental limitation of the sampling available from LEO satellites, which mostly vary in overpass time from late morning to early afternoon. Such platforms are ill suited for observing the diurnal cycles. Thus, inferences gleaned about aerosol distributions (and to the extent, radiative effects and air quality) cannot necessarily be transferred to other times of day. To remove this measurement gap on broader scales, it will be necessary to apply mature retrieval algorithms developed for LEO sensors to the second generation sensors in GEO (*cf.* Table 1), which are more capable, in terms of spectral and spatial coverage and radiometric data quality, to be used for the characterization of atmospheric composition and dynamics in air quality studies. With the aid from new microphysical schemes, advanced cloud ensemble models offer a quantitative means to connect satellite observations with ground-based measurements, furthering the understanding of aerosol-cloud-radiation interaction processes.

ACKNOWLEDGMENTS

The lead author thanks the continuous support of SMARTLabs deployment and research in Southeast Asia, as part of NASA Radiation Sciences Program (RSP) and Interdisciplinary Studies project. NASA EOS and RSP support deployments of AERONET and MPLNET. The authors thank the continuous support and assistance by the Taiwan Environmental Protection Administration (Contract No.: EPA-102-U1L1-02-101, EPA-103-U1L1-02-101, EPA-104-U1L1-02-101), and the Ministry of Science and Technology of Taiwan (Grant No. 103-2111-M-008-001, 104-2111-M-008-002). We also gratefully acknowledge the team efforts of logistic supports and assistance for instrument deployments provided by the National Central University (Taiwan), Vietnam Academy of Science and Technology (Vietnam, VAST.HTQT.NGA.04/15-16), National Hydro-Meteorological Service of Vietnam, Silpakorn University (Thailand), Chiang Mai University (Thailand), and the Doi Angkhang Meteorological Station (Thailand). Thanks are also given to all assistants and graduate students involving in the site operation, data analysis and technical support for making field campaigns successful.

APPENDIX: ACRONYM AND WEB LINKS

ABI: Advanced Baseline Imager, http://www.goes-r.gov/spacesegment/abi.html

AHI: Advanced Himawari Imager, http://www.data.jma.go.jp/mscweb/en/himawari89/space_segment/spsg_ahi.html

AIRS: Advanced Infrared Sounder, http://airs.jpl.nasa.gov/

ALADIN: Atmospheric LAser Doppler Instrument, http://www.esa.int/Our_Activities/Observing_the_Earth/The_Living_Planet_Programme/Earth_Explorers/ADM-Aeolus for the Atmospheric Dynamics Mission (ADM)

AMI: Advanced Meteoroligical Imager (no URL), sister instrument of ABI

ATLID: Atmospheric Lidar, http://www.esa.int/Our_Activities/Observing_the_Earth/The_Living_Planet_Programme/Earth_Explorers/EarthCARE/Payload for the EarthCARE mission

AVHRR: Advanced Very High Resolution Radiometer, http://noaasis.noaa.gov/NOAASIS/ml/avhrr.html

CALIOP: Cloud-Aerosol Lidar with Orthogonal Polarization, http://www.nasa.gov/mission_pages/calipso

CrIS: Cross-track Infrared Sounder, http://npp.gsfc.nasa.gov/cris.html

CPR: Cloud Profiling Radar, http://cloudsat.atmos.colostate.edu/ for the CloudSat mission

DPR: Dual-frequency Precipitation Radar, http://www.nasa.gov/mission_pages/GPM/main/ for Global Precipitation Measurement (GPM)

EPIC: Earth Polychromatic Imaging Camera, http://epic.gsfc.nasa.gov/ for the Deep Space Climate Observatory (DSCOVR)

FCI: Flexible Combined Imager, http://www.eumetsat.int/website/home/Satellites/FutureSatellites/MeteosatThirdGeneration/index.html

GEMS: Geostationary Earth Monitoring Spectrometer (no URL), sister instrument of TEMPO

GOCI: Geostationary Ocean Color Instrument, http://kosc.kiost.ac/kosc_web/GOCI_download/SatelliteData.html

GMI: GPM Microwave Imager, http://www.nasa.gov/mission_pages/GPM/main/ for Global Precipitation Measurement (GPM)

IASI: Infrared Atmospheric Sounding Interferometer, http://www.eumetsat.int/website/home/Satellites/CurrentSatellites/Metop/MetopDesign/IASI/index.html

MISR: Multiangle Imaging SpectroRadiometer, https://www-misr.jpl.nasa.gov/

MODIS: MODerate-resolution Imaging Spectroradiometer, http://modis-atmos.gsfc.nasa.gov/

OMI: Ozone Monitoring Instrument, http://aura.gsfc.nasa.gov/scinst/omi.html

OMPS: Ozone Mapping & Profiler Suite, http://npp.gsfc.nasa.gov/omps.html

POLDER: POlarization and Directionality of the Earth's Reflectances, https://polder-mission.cnes.fr/

SeaWiFS: Sea-viewing Wide Field-of-view Sensor, http://oceancolor.gsfc.nasa.gov

S-GLI: Second-generation GLobal Imager (no URL)

SLSTR: Sea and Land Surface Temperature Radiometer, https://sentinel.esa.int/web/sentinel/user-guides/sentinel-3-slstr/

SSM/I: Special Sensor Microwave Imager, http://www.remss.com/missions/ssmi

TEMPO: Tropospheric Emissions: Monitoring of POllution, http://science.nasa.gov/missions/tempo/

TROPOMI: TROPOspheric Monitoring Instrument, http://www.tropomi.eu/

UVNS: Ultra-Violet, Visible, Near infrared, Short wave infrared spectrometer, https://earth.esa.int/web/guest/missions/esa-future-missions/sentinel-5

VIIRS: Visible Infrared Imaging Radiometer Suite, http://npp.gsfc.nasa.gov/viirs.html

REFERENCES

Achtert, P., Birmili, W., Nowak, A., Wehner, B., Wiedensohler, A., Takegawa, N., Kondo, Y., Miyazaki, Y., Hu, M. and Zhu, T. (2009). Hygroscopic growth of tropospheric particle number size distributions over the North China Plain. *J. Geophys. Res.* 114: D00G07.

Andreae, M.O. and Merlet, P. (2001). Emission of trace gases and aerosols from biomass burning. *Global Biogeochem. Cycles* 15: 955–966.

Ansari, A.S. and Pandis, S.N. (2000). Water absorption by secondary organic aerosol and its effect on inorganic aerosol behavior. *Environ. Sci. Technol.* 34: 71–77.

Arola, A., Eck, T.F., Huttunen, J., Lehtinen, K.E.J., Lindfors, A.V., Myhre, G., Smirnov, A., Tripathi, S.N. and Yu, H. (2013). Influence of observed diurnal cycles of aerosol optical depth on aerosol direct radiative effect. *Atmos. Chem. Phys.* 13: 7895–7901.

Bai, Y., Suzuki, A.K. and Sagai, M. (2001). The cytotoxic effects of diesel exhaust particles on human pulmonary artery endothelial cells in vitro: Role of active oxygen species. *Free Radical Biol. Med.* 30: 555–562.

Bell, S.W., Hansell, R.A., Chow, J.C., Tsay, S.C., Hsu, N.C., Lin, N.H., Wang, S.H., Ji, Q., Li, C., Watson, J.G. and Khylstov, A. (2012). Constraining aerosol light extinction calculations of various air masses during 7-SEAS/Dongsha using collocated particle size and mass measurements. *Atmos. Environ.* 78: 163–173.

BéruBé, K., Balharry, D., Sexton, K., Koshy, L. and Jones, T. (2007). Combustion-derived nanoparticles: Mechanisms of pulmonary toxicity. *Clin. Exp. Pharmacol. Physiol.* 34: 1044–1050.

Brem, B.T., Mena Gonzalez, F.C., Meyers, S.R., Bond, T.C. and Rood, M.J. (2012). Laboratory-measured optical properties of inorganic and organic aerosols at relative humidities up to 95%. *Aerosol Sci. Technol.* 46: 178–190.

Carmichael, G.R., Adhikary, B., Kulkarni, S., D'Allura, A., Tang, Y., Streets, D., Zhang, Q., Bond, T.C., Ramanathan, V., Jamroensan, A. and Marrapu, P. (2009). Asian aerosols: Current and year 2030 distributions and implications to human health and regional climate change. *Environ. Sci. Technol.* 43: 5811–5817.

Carrico, C.M., Petters, M.D., Kreidenweis, S.M., Sullivan, A.P., McMeeking, G.R., Levin, E.J.T., Engling, G., Malm, W.C. and Collett Jr, J.L. (2010). Water uptake and chemical composition of fresh aerosols generated in open burning of biomass. *Atmos. Chem. Phys.* 10: 5165–5178.

Chambers, S.D., Kang, C.H., Williams, A.G., Crawford, J., Griffiths, A.D., Kim, K.H. and Kim, W.H. (2016). Improving the representation of cross-boundary transport of anthropogenic pollution in East Asia using Radon-222. *Aerosol Air Qual. Res.* 16: 958–976.

Chang, C.H., Hsiao, Y.L. and Hwang, C. (2015). Evaluating spatial and temporal variations of aerosol optical depth and biomass burning over Southeast Asia based on satellite data products. *Aerosol Air Qual. Res.* 15: 2625–2640.

Chang, S.S., Lee, W.J., Wang, L.C., Lin, N.H. and Chang-Chien, G.P. (2013). Influence of the Southeast Asian biomass burnings on the atmospheric persistent organic pollutants observed at near sources and receptor site. *Atmos. Environ.* 78: 184–194.

Chang, S.S., Lee, W.J., Holsen, T.M., Li, H.W., Wang, L.C. and Chang-Chien, G.P. (2014). Emissions of polychlorinated-*p*-dibenzo dioxin, dibenzofurans (PCDD/Fs) and polybrominated diphenyl ethers (PBDEs) from rice straw biomass burning. *Atmos. Environ.* 94: 573–581.

Chen, W.K., Li, T.C., Sheu, G.R., Lin, N.H., Chen, L.Y. and Yuan, C.S. (2016). Correlation analysis, transportation mode of atmospheric mercury and criteria air pollutants, with meteorological parameters at two remote sites of mountain and offshore island in Asia. *Aerosol Air Qual. Res.* 16: 2692–2705.

Chew, B.N., Campbell, J.R., Hyer, E.J., Salinas, S.V., Reid, J.S., Welton, E.J., Holben, B.N. and Liew, S.C. (2016). Relationship between aerosol optical depth and particulate matter over Singapore: Effects of aerosol vertical distributions. *Aerosol Air Qual. Res.* 16: 2818–2830.

Chew, T.L. and Bhatia, S. (2008). Catalytic processes towards the production of biofuels in a palm oil and oil palm biomass-based biorefinery. *Bioresour. Technol.* 99: 7911–7922.

Chi, K.H., Hung, N.T., Lin, C.Y., Wang, S.H., Ou-Yang, C.F., Lee, C.T. and Lin, N.H. (2016). Evaluation of atmospheric PCDD/Fs at two high-altitude stations in Vietnam and Taiwan during Southeast Asia biomass burning. *Aerosol Air Qual. Res.* 16: 2706–2715.

Chuang, H.C., Fan, C.W., Chen, K.Y., Chang-Chien, G.P. and Chan, C.C. (2012). Vasoactive alteration and inflammation induced by polycyclic aromatic hydrocarbons and trace metals of vehicle exhaust particles. *Toxicol. Lett*. 214: 131–136.

Chuang, H.C., Hsiao, T.C., Wang, S.H., Tsay, S.C. and Lin, N.H. (2016a). Characterization of particulate matter profiling and alveolar deposition from biomass burning in Northern Thailand: The 7-SEAS study. *Aerosol Air Qual. Res.* 16: 2897–2906.

Chuang, M.T., Fu, J.S., Lee, C.T., Lin, N.H., Gao, Y., Wang, S.H., Sheu, G.R., Hsiao, T.C., Wang, J.L., Yen, M.C., Lin, T.H. and Thongboonchoo, N. (2016b). The simulation of long-range transport of biomass burning plume and short-range transport of anthropogenic pollutants to a mountain observatory in East Asia during the 7-SEAS/2010 Dongsha Experiment. *Aerosol Air Qual. Res.* 16: 2933–2949.

Chuesaard, T., Chetiyanukornkul, T., Kameda, T., Hayakawa, K. and Toriba, A. (2014). Influence of biomass burning on the levels of atmospheric polycyclic aromatic hydrocarbons and their nitro derivatives in Chiang Mai, Thailand. *Aerosol Air Qual. Res.* 14: 1247–1257.

Crutzen, P.J. and Andreae, M.O. (1990). Biomass burning in the Tropics: Impact on atmospheric chemistry and biogeochemical cycles. *Science* 250: 1669–1678.

Dusek, U., Frank, G.P., Hildebrandt, L., Curtius, J., Schneider, J., Walter, S., Chand, D., Drewnick, F., Hings, S., Jung, D., Borrmann, S. and Andreae, M.O. (2006). Size matters more than chemistry for cloud nucleating ability of aerosol particles. *Science* 312: 1375–1378.

Dusek, U., Frank, G.P., Massling, A., Zeromskiene, K., Iinuma, Y., Schmid, O., Helas, G., Hennig, T., Wiedensohler, A. and Andreae, M.O. (2011). Water uptake by biomass burning aerosol at sub-and supersaturated conditions: Closure studies and implications for the role of organics. *Atmos. Chem. Phys.* 11: 9519–9532.

Engelhart, G.J., Hennigan, C.J., Miracolo, M.A., Robinson, A.L. and Pandis, S.N. (2012). Cloud condensation nuclei activity of fresh primary and aged biomass burning aerosol. *Atmos. Chem. Phys.* 12: 7285–7293.

Engling, G., Lee, J.J., Sie, H.J., Wu, Y.C. and I, Y.P. (2013). Anhydrosugar characteristics in biomass smoke aerosol—case study of environmental influence on particle-size of rice straw burning aerosol. *J. Aerosol Sci.* 54: 2–14.

EOS (Earth Observing System) (1999). *EOS Science Plan: The State of Science in the EOS Program*, King, M.D. (Ed.), NASA NP-1998-12-069-GSFC, 397pp.

Fu, P.Q., Kawamura, K., Chen, J., Li, J., Sun, Y.L., Liu, Y., Tachibana, E., Aggarwal, S.G., Okuzawa, K., Tanimoto, H., Kanaya, Y. and Wang, Z.F. (2012). Diurnal variations of organic molecular tracers and stable carbon isotopic composition in atmospheric aerosols over Mt. Tai in the North China Plain: An influence of biomass burning. *Atmos. Chem. Phys*. 12: 8359–8375.

Fujii, Y., Mahmud, M., Tohno, S., Okuda, T. and Mizohata, A. (2016). A case study of $PM_{2.5}$ characterization in Bangi, Selangor, Malaysia during the Southwest monsoon season. *Aerosol Air Qual. Res.* 16: 2685–2691.

Gautam, R., Hsu, N.C., Eck, T.F., Holben, B.N., Janjai, S., Jantarach, T., Tsay, S.C. and Lau, W.K.M. (2013). Characterization of aerosols over the Indochina peninsula from satellite-surface observations during biomass burning pre-monsoon season. *Atmos. Environ.* 78: 51–59.

Gupta, G.P., Kumar, B., Singh, S. and Kulshrestha, U.C. (2016). Deposition and impact of urban atmospheric dust on two medicinal plants during different seasons in NCR Delhi. *Aerosol Air Qual. Res.* 16: 2920–2932.

Hata, M., Chomanee, J., Thongyen, T., Bao, L., Tekasakul, S., Tekasakul, P., Otani, Y. and Furuuchi, M. (2014). Characteristics of nanoparticles emitted from burning of biomass fuels. *J. Environ. Sci*. 26: 1913–1920.

Hazucha, M.J., Bromberg, P.A., Lay, J.C., Bennett, W., Zeman, K., Alexis, N.E., Kehrl, H., Rappold, A.G., Cascio, W.E. and Devlin, R.B. (2013). Pulmonary responses in current smokers and ex-smokers following a two hour exposure at rest to clean air and fine ambient air particles. *Part. Fibre Toxicol.* 10: 58.

Hee, W.S., Lim, H.S., Mat Jafri, M.Z., Lolli, S. and Ying, K.W. (2016). Vertical profiling of aerosol types observed across monsoon seasons with a Raman lidar in Penang Island, Malaysia. *Aerosol Air Qual. Res.* 16: 2843–2854.

Hoff, R.M. and Christopher, S.A. (2009). Remote sensing of particulate pollution from space: have we reached the promised land? *J. Air Waste Manage. Assoc.* 59: 645–

675.

Holben, B.N., Eck, T.F., Slutsker, I., Tanré, D., Buis, J.P., Setzer, A., Vermote, E., Reagan, J.A., Kaufman, Y.J., Nakajima, T., Lavenu, F., Jankowiak, I. and Smirnov, A. (1998). AERONET: A federated instrument network and data archive for aerosol characterization. *Remote Sens. Environ.* 66: 1–16.

Holben, B.N. and Coauthors, (2016). Research at mesoscale and local scales of aerosol properties through the Distributed Regional Aerosol Gridded Observations Networks (DRAGON). Submitted to *Atmos. Chem. Phys. Dragon Special Issue*.

Hsiao, T.C., Ye, W.C., Wang, S.H., Tsay, S.C., Chen, W.N., Lin, N.H., Lee, C.T., Hung, H.M., Chuang, M.T. and Chantara, S. (2016). Investigation of the CCN activity, BC and UVBC mass concentrations of biomass burning aerosols during the 2013 BASELInE campaign. *Aerosol Air Qual. Res.* 16: 2742–2756.

Hsu, N.C., Herman, J.R. and Tsay, S.C. (2003). Radiative impacts from biomass burning in the presence of clouds during boreal spring in Southeast Asia. *Geophys. Res. Lett.* 30: 1224.

Hsu, N.C., Jeong, M.J., Bettenhausen, C., Sayer, A.M., Hansell, R.A., Seftor, C.S., Huang, J. and Tsay, S.C. (2013). Enhanced Deep Blue aerosol retrieval algorithm: The second generation. *J. Geophys. Res*. 118: 9296–9315.

IARC (International Agency for Research on Cancer) (2013). *Outdoor Air Pollution a Leading Environmental Cause of Cancer Deaths*. World Health Organization, Press Release on 17 Oct. 2013.

Idolor, L.F., de Guia, T.S., Francisco, N.A., Roa, C.C., Ayuyao, F.G., Tady, C.Z., Tan, D.T., Banal-Yang, S., Balanag, V.M. Jr., Reyes, M.T.N. and Dantes, R.B. (2011). Burden of obstructive lung disease in a rural setting in the Philippines. *Respirology* 16: 1111–1118.

IPCC (Intergovernmental Panel on Climate Change) (2013). *Climate Change 2013*: *The Physical Science Basis*. Contribution of Working Group I to the Fifth Assessment Report of the Intergovernmental Panel on Climate Change, Cambridge University Press, Cambridge, UK and New York, NY, USA, 1535 pp.

Jeong, M.J., Tsay, S.C., Ji, Q., Hsu, N.C., Hansell, R.A. and Lee, J. (2008). Ground-based measurements of airborne Saharan dust in marine environment during the NAMMA field experiment. *Geophys. Res. Lett.* 35: L20805.

Ji, Q. and Tsay, S.C. (2010). A novel non-intrusive method to resolve the thermal-dome-effect of pyranometers: Instrumentation and observational basis. *J. Geophys. Res.* 115: D00K21.

Ji, Q., Tsay, S.C., Lau, K.M., Hansell, R.A., Butler, J.J. and Cooper, J.W. (2011). A novel non-intrusive method to resolve the thermal-dome-effect of pyranometers: Radiometric calibration and implications. *J. Geophys. Res*. 116: D24105.

Khamkaew, C., Chantara, S., Janta, R., Pani, S.K., Prapamontol, T., Kawichai, S., Wiriya, W. and Lin, N.H. (2016). Investigation of biomass burning chemical components over Northern Southeast Asia during 7-SEAS/BASELInE 2014 campaign. *Aerosol Air Qual. Res.* 16: 2655–2670.

Khlystov, A., Stanier, C.O., Takahama, S. and Pandis, S.N. (2005). Water content of ambient aerosol during the Pittsburgh Air Quality Study. *J. Geophys. Res.* 110: D07S10.

Kim Oanh, N.T., Hang, N.T., Aungsiri, T., Worrarat, T. and Danutawat, T. (2016). Characterization of particulate matter measured at remote forest site in relation to local and distant contributing sources. *Aerosol Air Qual. Res.* 16: 2671–2684.

Klein, S.A. and Hartmann, D.L. (1993). The seasonal cycle of low stratiform clouds. *J. Clim.* 6: 1587–1606.

Kondo, Y., Matsui, H., Moteki, N., Sahu, L., Takegawa, N., Kajino, M., Zhao, Y., Cubison, M.J., Jimenez, J.L., Vay, S., Diskin, G.S., Anderson, B., Wisthaler, A., Mikoviny, T., Fuelberg, H.E., Blake, D.R., Huey, G., Weinheimer, A.J., Knapp, D.J. and Brune, W.H. (2011). Emissions of black carbon, organic, andinorganic aerosols from biomass burning in North America and Asia in 2008, *J. Geophys. Res*. 116: D08204.

Kusumaningtyas, S.D.A., Aldrian, E., Rahman, M.A. and Sopaheluwakan, A. (2016). Aerosol properties in Central Kalimantan due to peatland fire. *Aerosol Air Qual. Res.* 16: 2757–2767.

Lau, K.M. and Yang, S. (1997). Climatology and interannual variability of the southeast Asian summer monsoon. *Adv. Atmos. Sci*. 14: 141–162.

Lee, C.T., Ram, S.S., Nguyen, D.L., Chou, C.C.K., Chang, S.Y., Lin, N.H., Chang, S.C., Hsiao, T.C., Sheu, G.R., Ou-Yang, C.F., Chi, K.H., Wang, S.H. and Wu, X.C. (2016a). Aerosol chemical profile of near-source biomass burning smoke in Sonla, Vietnam during 7-SEAS campaigns in 2012 and 2013. *Aerosol Air Qual. Res.* 16: 2603–2617.

Lee, D., Sud, Y.C., Oreopoulos, L., Kim, K.M., Lau, W.K. and Kang, I.S. (2014). Modeling the influences of aerosols on pre-monsoon circulation and rainfall over Southeast Asia. *Atmos. Chem. Phys.* 14: 6853–6866.

Lee, J., Hsu, N.C., Bettenhausen, C., Sayer, A.M., Seftor, C.J., Jeong, M.J., Tsay, S.C., Welton, E.J., Wang, S.H. and Chen, W.N. (2016b). Evaluating the height of biomass burning smoke aerosols retrieved from synergistic use of multiple satellite sensors over Southeast Asia. *Aerosol Air Qual. Res.* 16: 2831–2842.

Lelieveld, J., Evans, J.S., Fnais, M., Giannadaki, D. and Pozzer, A. (2015). The contribution of outdoor air pollution sources to premature mortality on a global scale. *Nature* 525: 367–371.

Li, Z., Lau, W.K.M., Ramanathan, V., Wu, G., Ding, Y., Manoj, M.G., Liu, J., Qian, Y., Li, J., Zhou, T., Fan, J., Rosenfeld, D., Ming, Y., Wang, Y., Huang, J., Wang, B., Xu, X., Lee, S.S., Cribb, M., Zhang, F., Yang, X., Takemura, T., Wang, K., Xia, X., Yin, Y., Zhang, H., Guo, J., Zhai, P.M., Sugimoto, N., Babu, S.S. and Brasseur, G.P. (2016). Aerosol and monsoon climate interactions over Asia. *Rew. Geophys*. 54.

Lim, S.S., Vos, T., Flaxman, A.D., Danaei, G., Shibuya, K., *et al.* (2012). A comparative risk assessment of burden of disease and injury attributable to 67 risk

factors and risk factor clusters in 21 regions, 1990-2010: A systematic analysis for the Global Burden of Disease Study 2010. *Lancet* 380: 2224–2260.

Lin, N.H., Tsay, S.C., Maring, H.B., Yen, M.C., Sheu, G.R., Wang, S.H., Chi, K.H., Chuang, M.T., Ou-Yang, C.F., Fu, J.S., Reid, J.S., Lee, C.T., Wang, L.C., Wang, J.L., Hsu, C.N., Sayer, A.M., Holben, B.N., Chu, Y.C., Nguyen, X.A., Sopajaree, K., Chen, S.J., Cheng, M.T., Tsuang, B.J., Tsai, C.J., Peng, C.M., Schnell, R.C., Conway, T., Chang, C.T., Lin, K.S., Tsai, Y.I., Lee, W.J., Chang, S.C., Liu, J.J., Chiang, W.L., Huang, S.J., Lin, T.H. and Liu, G.R. (2013). Overview of regional experiments on biomass burning aerosols and related pollutants in Southeast Asia. *Atmos. Environ.* 78: 1–19.

Lin, N.H., Sayer, A.M., Wang, S.H., Loftus, A.M., Hsiao, T.C., Sheu, G.R., Hsu, N.C., Tsay, S.C. and Chantara, S. (2014). Interactions between biomass-burning aerosols and clouds over Southeast Asia: Current status, challenges, and perspectives. *Environ. Pollut*. 195: 292–307.

Loftus, A.M., Tsay, S.C., Pantina, P., Nguyen, C., Gabriel, P.M., Nguyen, X.A., Sayer, A.M., Tao, W.K. and Matsui, T. (2016). Coupled aerosol-cloud systems over Northern Vietnam during 7-SEAS/BASELInE: A radar and modeling perspective. *Aerosol Air Qual. Res.* 16: 2768–2785.

Löndahl, J., Massling, A., Swietlicki, E., Bräuner, E.V., Ketzel, M., Pagels, J. and Loft, S. (2009). Experimentally determined human respiratory tract deposition of airborne particles at a busy street. *Environ. Sci. Technol.* 43: 4659–4664.

Lyu, Y., Jaeger, C., Han, Z., Liu, L., Shi, P., Wang, W., Yang, S., Guo, L., Zhang, G., Hu, X., Guo, J., Gao, Y., Yang, Y., Xiong, Y., Wen, H., Liang, B. and Zhao, M. (2015). A severe air pollution event from field burning of agricultural residues in Beijing, China. *Aerosol Air Qual. Res.* 15: 2525–2536.

Martin, S.T., Artaxo, P., Machado, L.A.T., Manzi, A.O., Souza, R.A.F., Schumacher, C., Wang, J., Andreae, M.O., Barbosa, H.M.J., Fan, J., Fisch, G., Goldstein, A.H., Guenther, A., Jimenez, J.L., Pöschl, U., Silva Dias, M.A., Smith, J.N. and Wendisch, M. (2016). Introduction: Observations and modeling of the Green Ocean Amazon (GoAmazon2014/5). *Atmos. Chem. Phys.* 16: 4785–4797.

Martonen, T.B., Zhang, Z., Yue, G. and Musante, C. (2003). Fine particle deposition within human nasal airways. *Inhalation Toxicol.* 15: 283–304.

Molina, L.T., Madronich, S., Gaffney, J.S., Apel, E., de Foy, B., Fast, J., Ferrare, R., Herndon, S., Jimenez, J.L., Lamb, B., Osornio-Vargas, A.R., Russell, P., Schauer, J.J., Stevens, P.S., Volkamer, R. and Zavala, M. (2010). An overview of the MILAGRO 2006 Campaign: Mexico City emissions and their transport and transformation. *Atmos. Chem. Phys.* 10: 8697–8760.

Monn, C., Naef, R. and Koller, T. (2003). Reactions of macrophages exposed to particles <10 microm. *Environ. Res.* 91: 35–44.

Nguyen, D.L., Kawamura, K., Ono, K., Ram, S.S., Engling, G., Lee, C.T., Lin, N.H., Chang, S.C., Chuang, M.T., Hsiao, T.C., Sheu, G.R., Ou-Yang, C.F., Chi, K.H. and Sun, S.A. (2016). Comprehensive $PM_{2.5}$ organic molecular composition and stable carbon isotope ratios at Sonla, Vietnam: Fingerprint of biomass burning components. *Aerosol Air Qual. Res.* 16: 2618–2634.

Oozeer, M.Y., Chan, A., Ooi, M.C.G., Zarzur, A.M., Salinas, S.V., Chew, B.N., Morris, K.I. and Choong, W.K. (2016). Numerical study of the transport and convective mechanisms of biomass burning haze in South-Southeast Asia. *Aerosol Air Qual. Res.* 16: 2950–2963.

Paciorek, C.J. and Liu, Y. (2009). Limitations of remotely sensed aerosol as a spatial proxy for fine particulate matter. *Environ. Health Perspect.* 117: 904–909.

Pani, S.K., Wang, S.H., Lin, N.H., Tsay, S.C., Lolli, S., Chuang, M.T., Lee, C.T., Chantara, S. and Yu, J.Y. (2016a). Assessment of aerosol optical property and radiative effect for the layer decoupling cases over the northern South China Sea during the 7-SEAS/Dongsha experiment. *J. Geophys. Res.* 121: 4894–4906.

Pani, S.K., Wang, S.H., Lin, N.H., Lee, C.T., Tsay, S.C., Holben, B.N., Janjai, S., Hsiao, T.C., Chuang, M.T. and Chantara, S. (2016b). Radiative effect of springtime biomass-burning aerosols over Northern Indochina during 7-SEAS/BASELInE 2013 campaign. *Aerosol Air Qual. Res.* 16: 2802–2817.

Pantina, P., Tsay, S.C., Hsiao, T.C., Loftus, A.M., Kuo, F., Ou-Yang, C.F., Sayer, A.M., Wang, S.H., Lin, N.H., Hsu, N.C., Janjai, S., Chantara, S. and Nguyen, A.X. (2016). COMMIT in 7-SEAS/BASELInE: Operation of and observations from a novel, mobile laboratory for measuring in-situ properties of aerosols and gases. *Aerosol Air Qual. Res.* 16: 2728–2741.

Patterson, R.F., Zhang, Q., Zheng, M. and Zhu, Y. (2014). Particle deposition in respiratory tracts of school-aged children. *Aerosol Air Qual. Res*. 14: 64–73.

Pekour, M.S., Schmid, B., Chand, D., Hubbe, J.M., Kluzek, C.D., Nelson, D.A., Tomlinson, J.M. and Cziczo, D.J. (2012). Development of a new airborne humidigraph system. *Aerosol Sci. Technol.* 47: 201–207.

Penner, J.E., Dickinson, R.E. and O'Neill, C.A. (1992). Effects of aerosol from biomass burning on the global radiation budget. *Science* 256: 1432–1434.

Petters, M.D. and Kreidenweis, S.M. (2007). A single parameter representation of hygroscopic growth and cloud condensation nucleus activity. *Atmos. Chem. Phys.* 7: 1961–1971.

Petters, M.D., Carrico, C.M., Kreidenweis, S.M., Prenni, A.J., DeMott, P.J., Collett, J.L. and Moosmueller, H. (2009). Cloud condensation nucleation activity of biomass burning aerosol. *J. Geophys. Res.* 114: D22205.

Phan, V.T., Fink, A.H., Ngo-Duc, T., Trinh, T.L., Pinto, J.G., van der Linden, R. and Schubert, D. (2014). Observed climate variations and change in Vietnam. In *EWATEC-COAST: Technologies for Environmental and Water Protection of Coastal Zones in Vietnam*, Meon, P. and Van Phuoc, N. (Eds.), Contributions to the 4th International Conference for Environment and Natural Resources, ICENR 2014, Cuvillier, Göttingen, Germany.

Pongpiachan, S. (2016). Incremental lifetime cancer risk of

$PM_{2.5}$ bound polycyclic aromatic hydrocarbons (PAHs) before and after the wildland fire episode. *Aerosol Air Qual. Res.* 16: 2907–2919.

Popovicheva, O.B., Engling, G., Diapouli, E., Saraga, D., Persiantseva, N.M., Timofeev, M.A., Kireeva, E.D., Shonija, N.K., Chen, S.H., Nguyen, D.L., Eleftheriadis, K. and Lee, C.T. (2016). Impact of smoke intensity on size-resolved aerosol composition and microstructure during the biomass burning season in Northwest Vietnam. *Aerosol Air Qual. Res.* 16: 2635–2654.

Qi, B., Hu, D., Che, H., Du, R., Wu, Y., Xia, X., Zha, B., Liu, J., Niu, Y., Wang, H., Zhang, D. and Shi, G. (2016). Seasonal variation of aerosol optical properties in an urban site of the Yangtze Delta Region of China. *Aerosol Air Qual. Res.* 16: 2884–2896.

Redemann, J., Russell, P.B. and Hamill, P. (2001). Dependence of aerosol light absorption and single-scattering albedo on ambient relative humidity for sulfate aerosols with black carbon cores. *J. Geophys. Res.* 106: 27485–27495.

Reid, J.S., Hyer, E.J., Johnson, R.S., Holben, B.N., Yokelson, R.J., Zhang, J., Campbell, J.R., Christopher, S.A., Di Girolamo, L., Giglio, L., Holz, R.E., Kearney, C., Miettinen, J., Reid, E.A., Turk, F.J., Wang, J., Xian, P., Zhao, G., Balasubramanian, R., Chew, B.N., Janjai, S., Lagrosas, N., Lestari, P., Lin, N.H., Mahmud, M., Nguyen, A.X., Norris, B., Oanh, N.T.K., Oo, M., Salinas, S.V., Welton, E.J. and Liew, S.C. (2013). Observing and understanding the Southeast Asian aerosol system by remote sensing: An initial review and analysis for the Seven Southeast Asian Studies (7SEAS) program. *Atmos. Res*. 122: 403–468.

Reutter, P., Su, H., Trentmann, J., Simmel, M., Rose, D., Gunthe, S.S., Wernli, H., Andreae, M.O. and Pöschl, U. (2009). Aerosol- and updraft-limited regimes of cloud droplet formation: Influence of particle number, size and hygroscopicity on the activation of cloud condensation nuclei (CCN). *Atmos. Chem. Phys.* 9: 7067–7080.

Rissler, J., Swietlicki, E., Zhou, J., Roberts, G., Andreae, M.O., Gatti, L.V. and Artaxo, P. (2004). Physical properties of the sub-micrometer aerosol over the Amazon rain forest during the wet-to-dry season transition-comparison of modeled and measured CCN concentrations. *Atmos. Chem. Phys.* 4: 2119–2143.

Rissler, J., Vestin, A., Swietlicki, E., Fisch, G., Zhou, J., Artaxo, P. and Andreae, M.O. (2006). Size distribution and hygroscopic properties of aerosol particles from dry-season biomass burning in Amazonia. *Atmos. Chem. Phys.* 6: 471–491.

Sayer, A.M., Hsu, N.C., Bettenhausen, C., Lee, J., Redemann, J., Schmid, B. and Shinozuka, Y. (2016a). Extending *Deep Blue* aerosol retrieval coverage to cases of absorbing aerosols above clouds: Sensitivity analysis and first case studies. *J. Geophys. Res*. 121: 4830–4854.

Sayer, A.M., Hsu, N.C., Hsiao, T.C., Pantina, P., Kuo, F., Ou-Yang, C.F., Holben, B.N., Janjai, S., Chantara, S., Wang, S.H., Loftus, A.M., Lin, N.H. and Tsay, S.C. (2016b). In-situ and remotely-sensed observations of biomass burning aerosols at Doi Ang Khang, Thailand during 7-SEAS/BASELInE 2015. *Aerosol Air Qual. Res.* 16: 2786–2801.

Schmidt-Thomé, P., Nguyen, T.H., Pham, T.L., Jarva, J. and Nuottimäki, K. (2015). *Climate Change Adaptation Measures in Vietnam*. Development and Implementation, Springer International Publishing, 100pp.

Seaton, A., MacNee, W., Donaldson, K. and Godden, D. (1995). Particulate air pollution and acute health effects. *Lancet* 345: 176–178.

Sevimoglu, O. and Rogge, W.F. (2015). Organic compound concentrations of size-segregated PM_{10} during sugarcane burning and growing seasons at a rural and an urban site in Florida, USA. *Aerosol Air Qual. Res.* 15: 1720–1736.

Squadrito, G.L., Cueto, R., Dellinger, B. and Pryor, W.A. (2001). Quinoid redox cycling as a mechanism for sustained free radical generation by inhaled airborne particulate matter. *Free Radical Biol. Med.* 31: 1132–1138.

Tian, S., Pan, Y., Liu, Z., Wen, T. and Wang, Y. (2014). Size-resolved aerosol chemical analysis of extreme haze pollution events during early 2013 in urban Beijing, China. *J. Hazard. Mater*. 279: 452–460.

Titos, G., Lyamani, H., Cazorla, A., Sorribas, M., Foyo-Moreno, I., Wiedensohler, A. and Alados-Arboledas, L. (2014). Study of the relative humidity dependence of aerosol light-scattering in southern Spain. *Tellus Ser. B* 66: 24536.

Tiwari, M., Sahu, S.K. and Pandit, G.G. (2015). Inhalation risk assessment of PAH exposure due to combustion aerosols generated from household fuels. *Aerosol Air Qual. Res.* 15: 582–590.

Tsay, S.C., Hsu, N.C., Lau, W.K.M., Li, C., Gabriel, P.M., Ji, Q., Holben, B.N., Judd Welton, E., Nguyen, A.X., Janjai, S., Lin, N.H., Reid, J.S., Boonjawat, J., Howell, S.G., Huebert, B.J., Fu, J.S., Hansell, R.A., Sayer, A.M., Gautam, R., Wang, S.H., Goodloe, C.S., Miko, L.R., Shu, P.K., Loftus, A.M., Huang, J., Kim, J.Y., Jeong, M.J. and Pantina, P. (2013). From BASE-ASIA towards 7-SEAS: A satellite-surface perspective of boreal spring biomass-burning aerosols and clouds in Southeast Asia. *Atmos. Environ.* 78: 20–34.

Turekian, V.C., Macko, S.A. and Keene, W.C. (2003). Concentrations, isotopic compositions, and sources of size-resolved, particulate organic carbon and oxalate in near-surface marine air at Bermuda during spring. *J. Geophys. Res*. 108: 4157.

van Donkelaar, A., Martin, R.V., Brauer, M., Kahn, R., Levy, R., Verduzco, C. and Villeneuve, P.J. (2010). Global estimates of ambient fine particulate matter concentrations from satellite-based aerosol optical depth: Development and application. *Environ. Health Perspect.* 118: 847–855.

van Donkelaar, A., Martin, R.V., Brauer, M. and Boys, B.L. (2014). Use of satellite observations for long-term exposure assessment of global concentrations of fine particulate matter. *Environ. Health Perspect.* 123: 847–855.

Wang, J. and Martin, S.T. (2007). Satellite characterization of urban aerosols: Importance of including hygroscopicity

and mixing state in the retrieval algorithms. *J. Geophys. Res.* 112: D17203.

Wang, S.H., Welton, E.J., Holben, B.N., Tsay, S.C., Lin, N.H., Giles, D., Stewart, S.A., Janjai, S., Nguyen, A.X., Hsiao, T.C., Chen, W.N., Lin, T.H., Buntoung, S., Chantara, S. and Wiriya, W. (2015). Vertical distribution and columnar optical properties of springtime biomass-burning aerosols over northern Indochina during 2014 7-SEAS campaign. *Aerosol Air Qual. Res.* 15: 2037–2050.

Wang, Z., Chen, L., Tao, J., Liu, Y., Hu, X. and Tao, M. (2014). An empirical method of RH correction for satellite estimation of ground-level PM concentrations. *Atmos. Environ.* 95: 71–81.

Welton, E.J., Voss, K.J., Quinn, P.K., Flatau, P.J., Markowicz, K., Campbell, J.R., Spinhirne, J.D., Gordon, H.R. and Johnson, J.E. (2002). Measurements of aerosol vertical profiles and optical properties during INDOEX 1999 using micropulse lidars, *J. Geophys. Res*. 107: 8019.

Welton, E.J., Campbell, J.R., Spinhirne, J.D. and Scott, V.S. (2001). Global Monitoring of Clouds and Aerosols Using a Network of Micro-pulse Lidar Systems, In *Lidar Remote Sensing for Industry and Environmental Monitoring*, Singh, U.N., Itabe, T. and Sugimoto, N. (Eds.), Proc. SPIE, 4153, pp. 151–158.

West, R.E.L., Stier, P., Jones, A., Johnson, C.E., Mann, G.W., Bellouin, N., Partridge, D.G. and Kipling, Z. (2014). The importance of vertical velocity variability for estimates of the indirect aerosol effects. *Atmos. Chem. Phys.* 14: 6369–6393.

Wielicki, B.A., Wong, T., Allan, R.P., Slingo, A., Kiehl, J.T., Soden, B.J., Gordon, C.T., Miller, A.J., Yang, S.K., Randall, D.A., Robertson, F., Susskind, J. and Jacobowitz, H. (2002). Evidence for large decadal variability in the tropical mean radiative energy budget. *Science* 295: 841–844.

Winker, D.M., Vaughan, M.A., Omar, A., Hu, Y., Powell, K.A., Liu, Z., Hunt, W.H. and Young, S.A. (2009). Overview of the CALIPSO mission and CALIOP data processing algorithms. *J. Atmos. Oceanic Technol.* 26: 2310–2323.

Wiriya, W., Chantara, S., Sillapapiromsuk, S. and Lin, N.H. (2016). Emission profiles of PM_{10}-bound polycyclic aromatic hydrocarbons from biomass burning determined in chamber for assessment of air pollutants from open burning. *Aerosol Air Qual. Res.* 16: 2716–2727.

Wood, R. (2012). Review: Stratocumulus clouds. *Mon. Weather Rev.* 140: 2373–2423.

Wozniak, A.S., Bauer, J.E., Dickhut, R.M., Xu, L. and McNichol, A.P. (2012). Isotopic characterization of aerosol organic carbon components over the eastern United States. *J. Geophys. Res.* 117: D13303.

Yen, M.C., Peng, C.M., Chen, T.C., Chen, C.S., Lin, N.H., Tzeng, R.Y., Lee, Y.A. and Lin, C.C. (2013). Climate and weather characteristics in association with the active fires in northern Southeast Asia and spring air pollution in Taiwan during 2010 7-SEAS/Dongsha Experiment. *Atmos. Environ.* 78: 35–50.

Zieger, P., Fierz-Schmidhauser, R., Weingartner, E. and Baltensperger, U. (2013). Effects of relative humidity on aerosol light scattering: Results from different European sites. *Atmos. Chem. Phys.* 13: 10609–10631.

Received for review, August 9, 2016
Revised, October 21, 2016
Accepted, October 25, 2016